Dissertationes Forestales 335

Unravelling $\delta^{13}C$ signal in Scots pine trees for climate change and tree physiology studies

Yu Tang

Institute for Atmospheric and Earth System Research / Forest Sciences,

Faculty of Agriculture and Forestry

University of Helsinki

Academic dissertation

To be presented for public discussion with the permission of the Faculty of Agriculture and Forestry of the University of Helsinki on the 23th of February, 2023 at 10 o'clock.

The defence is open for audience through remote access.

Helsinki 2023

Title of dissertation: Unravelling $\delta^{13}C$ signal in Scots pine trees for climate change and tree physiology studies
Author: Yu Tang

Dissertationes Forestales 335
https://doi.org/10.14214/df.335

Thesis Supervisors:
Dr. Katja T. Rinne-Garmston
Bioeconomy and Environment Unit, Natural Resources Institute Finland (Luke)

Professor Jaana Bäck
Institute for Atmospheric and Earth System Research / Forest Sciences, Faculty of Agriculture and Forestry, University of Helsinki, Finland

Dr. Pauliina Schiestl-Aalto
Institute for Atmospheric and Earth System Research / Physics, Faculty of Science, University of Helsinki, Finland

Pre-examiners:
Dr. Lisa Wingate
National Research Institute for Agriculture, Food and Environment (INRAE), Bordeaux Sciences Agro, UMR ISPA, Villenave d'Ornon 33140, France

Dr. Roland A. Werner
Institute of Agricultural Sciences, ETH Zurich, Zurich, Switzerland

Opponent:
Associate Professor Lucas A. Cernusak
College of Science and Engineering, James Cook University, Cairns, Australia

ISSN 1795-7389 (online)
ISBN 978-951-651-760-8 (pdf)

Publishers:
Finnish Society of Forest Science
Faculty of Agriculture and Forestry of the University of Helsinki
School of Forest Sciences of the University of Eastern Finland

Editorial Office:
Finnish Society of Forest Science
Viikinkaari 6, 00790 Helsinki, Finland
https://www.dissertationesforestales.fi

Tang, Y. (2023). Unravelling $\delta^{13}C$ signal in Scots pine trees for climate change and tree physiology studies. Dissertationes Forestales 335. 54 p.
https://doi.org/10.14214/df.335

ABSTRACT

Stable carbon isotope composition ($\delta^{13}C$) in trees responds sensitively to the changing environmental conditions and thus provides a powerful tool for paleoenvironmental reconstructions. The retrospective interpretation of tree $\delta^{13}C$ signal depends on comprehensive understanding of how environmental and physiological signals are recorded in $\delta^{13}C$ during photosynthesis and how the $\delta^{13}C$ signal is modified after photosynthesis.

This thesis aims to improve the understanding of photosynthetic and post-photosynthetic isotope fractionation processes, and to examine the suitability of tree-ring $\delta^{13}C$ for intra-seasonal reconstructions of intrinsic water use efficiency (iWUE). The former goal was studied by combining compound-specific isotope analysis of organic matter with isotope discrimination models and online $\delta^{13}C$ measurements of leaf CO_2 fluxes for field-grown mature Scots pine (*Pinus sylvestris* L.). The latter was achieved via comparing 18-year-long intra-seasonal iWUE chronologies estimated from laser ablation derived tree-ring $\delta^{13}C$, gas exchange and eddy covariance data.

Mesophyll conductance and time-integral effect of leaf assimilates had a clear impact on the intra-seasonal dynamics of leaf sugar $\delta^{13}C$. No significant use of reserves was observed for biomass growth of needles, stem or roots of Scots pine. Unlike sucrose, leaf bulk matters had significant $\delta^{13}C$ offsets from new assimilates, leading to distorted environmental and physiological signals documented in their $\delta^{13}C$. The reliability of tree-ring $\delta^{13}C$ data for intra-seasonal iWUE reconstructions was supported by an agreement of intra-seasonal patterns across the iWUE estimation methods.

These results broaden our knowledge of the less well-known photosynthetic and post-photosynthetic isotopic fractionation processes, demonstrate the benefits of analysing sucrose $\delta^{13}C$ for understanding plant physiological responses, and show that the tree-ring $\delta^{13}C$-based iWUE reconstructions can be extended to intra-seasonal scale. This information not only helps to better unravel $\delta^{13}C$ signal in trees, but also improves reliable reconstructions of environmental and physiological signals from tree-ring $\delta^{13}C$.

Keywords: photosynthetic and post-photosynthetic isotope discrimination, intrinsic water use efficiency (iWUE), boreal forests, compound-specific isotope analysis (CSIA), laser ablation

ACKNOWLEDGEMENTS

One day five years ago, I was sitting in front of Katja and was nervous in my PhD interview. Suddenly, a ray of sun came through the shutters and hit my face. That moment, I had the sense that my PhD journey would be full of warmth, happiness and hope. Indeed, through the years I have received so much help, kindness and support, without which I could not finish this thesis.

First, I want to express my deepest gratitude to my supervisor Dr. Katja Rinne-Garmston. Thank you for guiding me to such a fascinating research area, offering me the chance to conduct fieldwork in the breathtaking Finnish forests, hands-on teaching me field and laboratory work, encouraging me to present my research on various occasions, inspiring my critical thinking and scientific reasoning skills, and giving me enormous support whenever it is needed. My sincere thanks also go to my co-supervisors Prof. Jaana Bäck and Dr. Pauliina Schielst-Aalto. Thank you Jaana for patient guidance through my graduation and continuous support during manuscript writing. Thank you Pauliina for the help in fieldwork and modelling, prompt response to my questions and queries, and being excited about my results.

I appreciate Dr. Roland A. Werner and Dr. Lisa Wingate for their time to pre-examine this thesis, Assoc. Prof. Lucas A. Cernusak for agreeing to be my opponent, and Prof. Paula Elomaa for being a member of my grading committee. I also thank my thesis committee, Prof. Timo Vesala and Dr. Harri Mäkinen, for their constructive suggestions on the progress of my doctoral study. Additionally, this thesis would not have been completed without financial support by the European Research Council (grant no. 755865), the Academy of Finland (grant no. 295319) and the Finnish Cultural Foundation (grant no. 00221014).

I am very grateful to Dr. Elina Sahlstedt for her help in fieldwork and isotope analysis, and warm encouragements all the time. I am also thankful to the other ISOBOREAL members, Dr. Giles Young, Dr. Kersti Leppä, Dr. Charlotte Angove, Dr. Petri Kilpeläinen and Dr. Bartosz Adamczyk for inspiring discussions and help in field and laboratory work. Thanks should also go to my collaborators, Dr. Matthias Saurer and Dr. Marco M. Lehmann at WSL, Dr. Pasi Kolari, Dr. Liisa Kulmala, Dr. Kira Ryhti, Dr. Yann Salmon and Dr. Yiyang Ding at University of Helsinki, and Dr. Tuula Jyske at Luke, for their invaluable contributions to the manuscripts.

I would like to extend my sincere thanks to the summer and intern students, who are Esko Karvinen, Aino Ovaska, Salla Kuittinen, Jukka Kärki, Aino Seppänen, Marine Manche, Fana Teferra, Antti Tiisanoja and Nikol Ilchevska, and to the technical staffs, who are Ari Kinnunen, Natalia Kiuru, Anneli Rautiainen and Kaarina Pynnönen at Luke and Manuela Oettli at WSL, for their help in field and laboratory work. Special thanks to the people at SMEAR stations in Hyytiälä and Värriö for maintaining the stations that support this study. My appreciation also goes to Dr. Kari Minkkinen for his help in abstract translation.

I also thank my Luke colleagues for their kindness and inspiring talks. Warm thanks to Manqing, Wenzi, Man Hu, Jiayi, Lili, Aruo and many other friends I met in board games.

Lastly, I want to thank my family for being my safe haven. Special thanks to Shuzhi, my daughter, for easing all the anxiety that appeared at the end of my doctoral period, and Yulong, my love, for constant support and love.

LIST OF ORIGINAL ARTICLES

This dissertation is based on the following articles (referred to in the text by their Roman numbers):

I **Tang Y.**, Schiestl-Aalto P., Lehmann M.M., Saurer M., Sahlstedt E., Kolari P., Leppä K., Bäck J., Rinne-Garmston K.T. (2023). Estimating the intra-seasonal photosynthetic discrimination and water use efficiency using $\delta^{13}C$ of leaf sucrose. Journal of Experimental Botany, 74, 321–335. https://doi.org/10.1093/jxb/erac413

II Leppä K., **Tang Y.**, Ogée J., Launiainen S., Kahmen A., Kolari P., Sahlstedt E., Saurer M., Schiestl-Aalto P., Rinne-Garmston K.T. (2022). Explicitly accounting for needle sugar pool size crucial for predicting intra-seasonal dynamics of needle carbohydrates $\delta^{18}O$ and $\delta^{13}C$. New Phytologist, 236, 2044–2060. https://doi.org/10.1111/nph.18227

III **Tang Y.**, Schiestl-Aalto P., Saurer M., Sahlstedt E., Kulmala L., Kolari P., Ryhti K., Jyske T., Ding Y., Salmon Y., Bäck J., Rinne-Garmston K.T. (2022). Tree organ growth and carbon allocation dynamics impact the magnitude and $\delta^{13}C$ signal of stem and soil CO_2 fluxes. Tree Physiology, 42, 2404–2418. https://doi.org/10.1093/treephys/tpac079

IV **Tang Y.**, Sahlstedt E., Young G., Schiestl-Aalto P., Saurer M., Kolari P., Jyske T., Bäck J., Rinne-Garmston K.T. (2022). Estimating intraseasonal intrinsic water-use efficiency from high-resolution tree-ring $\delta^{13}C$ data in boreal Scots pine forests. New Phytologist. http://doi.org/10.1111/nph.18649

AUTHOR'S CONTRIBUTION

I	YT contributed to the conceptualization of the study with the lead of KR-G, participated in the fieldwork, and had the main responsibility in laboratory preparation of samples, data analysis, result interpretation and manuscript writing.
II	YT participated in fieldwork, lead the laboratory preparation of samples, and participated in data analysis, result interpretation and manuscript writing.
III	YT contributed to the conceptualization of the study with the lead of KR-G, participated in the fieldwork, and had the main responsibility in laboratory preparation of samples, data analysis, result interpretation and manuscript writing.
IV	YT conceived the study with KR-G, participated in fieldwork, and had the main responsibility in data analysis, result interpretation and manuscript writing.

TABLE OF CONTENTS

SYMBOLS AND ABBREVIATIONS

a_b	fractionation factor associated with diffusion through the boundary layer
a_m	fractionation factor associated with transfer through mesophyll
A_n	net assimilation rate
a_s	fractionation factor associated with diffusion through stomata
b	fractionation factor associated with carboxylation
C_a	CO_2 concentration in ambient air
C_c	CO_2 concentration in the chloroplasts
C_i	CO_2 concentration in the intercellular air spaces
C_s	CO_2 concentration at the leaf surface
CSIA	compound-specific isotope analysis
Δ	carbon isotope discrimination
$\delta^{13}C$	stable carbon isotope composition
$\delta^{13}C_A$	$\delta^{13}C$ of assimilates
$\delta^{13}C_{air}$	$\delta^{13}C$ of ambient CO_2
$\delta^{13}C_i$	$\delta^{13}C$ of intercellular CO_2
$\delta^{13}C_{sub}$	$\delta^{13}C$ of respiratory substrate
e	fractionation factor associated with mitochondrial respiration
E	water vapor flux out of leaves
e^*	apparent fractionation factor if respiratory substrate is not new assimilates
ET	evapotranspiration or ecosystem H_2O flux
f	fractionation factor associated with photorespiration

Γ_*	CO_2 compensation point in the absence of dark respiration
g_b	boundary layer conductance
g_m	mesophyll conductance
GPP	gross primary production
g_s	stomatal conductance
HPLC	high-performance liquid chromatography
IRMS	isotope ratio mass spectrometry
iWUE	intrinsic water use efficiency
$iWUE_{EC}$	intrinsic water use efficiency derived from eddy covariance data
$iWUE_{gas}$	intrinsic water use efficiency derived from leaf gas exchange data
$iWUE_{iso}$	intrinsic water use efficiency derived from carbon isotope composition data
k	carboxylation efficiency
LA	laser ablation
P_a	atmospheric pressure
PAR	photosynthetically active radiation
PEPc	phospho*enol*pyruvate carboxylase
R_d	day respiration rate
RH	relative humidity
Rubisco	ribulose 1,5-bisphosphate carboxylase/oxygenase
T	temperature
TOM	total organic matter
VPD	vapor pressure deficit
WSCs	water soluble carbohydrates (sugars + pinitol/myo-inositol)
WSOM	water-soluble organic matter

1. INTRODUCTION

Boreal forests cover 30% of the global forest area, store over 30% of global terrestrial carbon and account for ca. 20% of the total carbon sink sequestrated by the world's forests (Gauthier et al. 2015). However, carbon uptake and sequestration of the boreal biome is being strongly impacted by the changing climate. The increased temperature and prolonged growing season length have been suggested to contribute to the enhanced forest production, for example, in Fennoscandia (Kauppi et al. 2014) and over major regions of Russia (Lapenis et al. 2005). A potential shift to a drier climate (Gauthier et al. 2015) and more frequent drought events (Peng et al. 2011) in the boreal forest regions, on the contrary, may pose adverse effects on forest growth. Central to the consequences of climate change on boreal forest productivity is how trees respond to the changing local environmental conditions, which is, however, still poorly understood.

Stable carbon isotope composition ($\delta^{13}C$) in trees has proven to be a powerful tool to study the response of trees to changes in the environment where the trees live. The $\delta^{13}C$ signal is originally recorded in leaf assimilates and then transferred to other parts of the trees, eventually archived in tree organic matter, released back to the atmosphere via respiration or transported to soil via mycorrhizal fungi (Bowling et al. 2008). Following $\delta^{13}C$ signal within trees can help to decipher the impact of environmental factors on the $\delta^{13}C$ signal of tree biomass and respired CO_2. With this knowledge, the $\delta^{13}C$ preserved in tree-rings can be used to backtrack physiological responses of trees to climate change in the past, which allows us to better predict the response of forests to climate change in the future.

1.1 Recording $\delta^{13}C$ signal in leaf assimilates

Carbon has two stable isotopes, ^{12}C and ^{13}C, which both have six protons but differ in the number of neutrons. Although the two isotopes have almost identical chemical properties, their difference in mass causes discrimination against one of them during physical, chemical and biological processes, consequently imparting an environmental signal. The ratio of ^{13}C to ^{12}C is by convention expressed in delta (δ) notation, in per mil (‰), relative to an international standard (Vienna-Pee Dee Belemnite, VPDB) (Eq. 1).

$$\delta^{13}C=(R_{sample}/R_{standard} - 1) \cdot 1000, \quad (1)$$

where R_{sample} and $R_{standard}$ are the $^{13}C/^{12}C$ ratios in a sample and standard, respectively. For example, the $\delta^{13}C$ of atmospheric CO_2 (hereafter $\delta^{13}C_{air}$) is ca. -8‰, indicating a lower ^{13}C content in air CO_2 relative to the standard. Although carbon in trees has its origin in the atmospheric CO_2, $\delta^{13}C$ of tree organic matter is significantly lower than $\delta^{13}C_{air}$. This is mainly because trees discriminate against ^{13}C during photosynthetic CO_2 fixation and metabolic processes after photosynthesis, thus yielding different and varying $\delta^{13}C$ values in leaf assimilates and downstream metabolites. This difference in $\delta^{13}C$ from source (air CO_2) to product (leaf assimilates) can be defined as carbon isotope discrimination (Δ, Eq.2):

$$\Delta=(\delta^{13}C_{air} - \delta^{13}C_A)/(1 + \delta^{13}C_A), \quad (2)$$

where $\delta^{13}C_A$ is $\delta^{13}C$ of assimilates.

There are three common ways to estimate $\delta^{13}C_A$. First, $\delta^{13}C$ of tree biomass, as determined by isotope ratio mass spectrometry (IRMS), is conventionally regarded as an integrated signal of $\delta^{13}C_A$ over the period of tissue synthesis (Cernusak et al. 2013). Compared with bulk biomass, leaf carbohydrates or individual sugars provide a more precise estimation of $\delta^{13}C_A$, because of their relatively closer relation to new assimilates (Bögelein et al. 2019). Second, $\delta^{13}C_A$ can be derived from online $\delta^{13}C$ analysis of the CO_2 flux entering and leaving a leaf gas exchange chamber connected to an optical spectrometer, such as a tunable diode laser absorption spectrometer (Wingate et al. 2010) or a cavity ring-down spectrophotometer (Schiestl-Aalto et al. 2021). Third, $\delta^{13}C_A$ can be estimated via isotope discrimination models, such as the classic model developed by Farquhar et al. (1982) and its advanced versions (Wingate et al. 2007; Farquhar and Cernusak 2012; Busch et al. 2020). The accuracy of the model results relies on profound understanding of fractionation processes involved in leaf photosynthesis.

1.1.1 Underlying mechanisms for photosynthetic isotope fractionation

Photosynthetic carbon uptake of C3 plants (including most tree species) reflects the balance between CO_2 supply and CO_2 demand, which are limited by CO_2 diffusion from the ambient air to the site of carboxylation and the rates of carboxylation, day respiration and photorespiration. As a result, the value of Δ is a net effect of isotope fractionations occurring in all these processes (Figure 1).

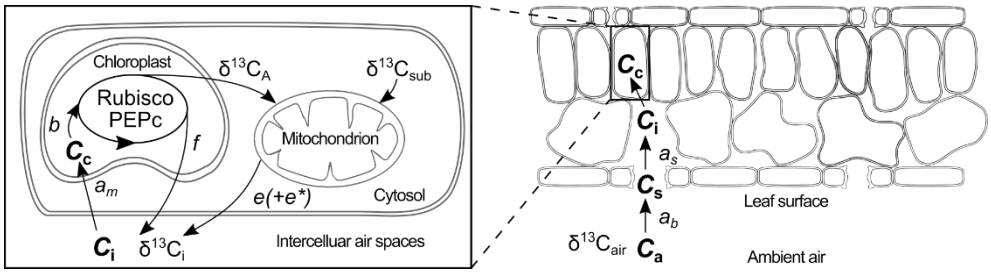

Figure 1. Conceptual diagram showing the flow of carbon during photosynthetic uptake and the associated fractionation processes (modified after Wingate et al. 2007). a_b, a_s, a_m, b, f, e and e^* are the (apparent) fractionation factors associated with diffusion through the boundary layer, diffusion through stomata, transfer through mesophyll, carboxylation catalyzed by ribulose 1,5-bisphosphate carboxylase/oxygenase (Rubisco) or phospho*enol*pyruvate carboxylase (PEPc), photorespiration, mitochondrial respiration feeding on new assimilates, mitochondrial respiration feeding on other substrates, respectively; C_a, C_s, C_i and C_c are the CO_2 concentration in ambient air, at the leaf surface, in the intercellular air spaces and in the chloroplasts, respectively; $\delta^{13}C_{air}$, $\delta^{13}C_i$, $\delta^{13}C_A$ and $\delta^{13}C_{sub}$ are the carbon isotope compositions of ambient CO_2, intercellular CO_2, new assimilates and respiratory substrates other than new assimilates.

The first source of photosynthetic discrimination occurs during the diffusion of CO_2 from the ambient air to the leaf surface, governed by boundary layer conductance (g_b). Since the diffusivity of $^{13}CO_2$ molecules is less than that of $^{12}CO_2$ in air (Farquhar et al. 1982), air at the leaf surface is depleted in ^{13}C relative to ambient air. The fractionation factor associated with diffusion through the laminar boundary layer (a_b) is well acknowledged as 2.9‰ (Farquhar 1983). However, the effect of g_b on Δ and $\delta^{13}C_A$ is usually insignificant under experimental conditions (Seibt et al. 2008), given that the value of g_b is large in well stirred gas exchange chambers (Uddling and Wallin 2012). Even under field conditions, g_b is often an order of magnitude greater than stomatal conductance (g_s) (Ogée et al. 2003), and therefore has a relatively small impact on the magnitude of Δ and $\delta^{13}C_A$.

Similarly, as $^{12}CO_2$ in air diffuses more easily than $^{13}CO_2$ through stomata, the internal air is even more depleted in ^{13}C relative to air at the leaf surface, causing a fractionation factor due to diffusion (a_s) of 4.4‰ (Farquhar et al. 1982). The discrimination associated with g_s is inversely related to the ratio of intercellular to ambient CO_2 concentrations (C_i/C_a). If g_s is extremely low and little CO_2 enters the leaf, the C_i/C_a approaches 0 and Δ is strongly determined by g_s with a value tending towards 4.4‰. Conversely, if g_s is comparatively high, the C_i/C_a gets close to 1 and the impact of g_s on Δ becomes negligible. As the C_i/C_a is a function of CO_2 supply to the intercellular air spaces and CO_2 demand (Cernusak et al. 2013), which are impacted by g_s and photosynthetic rate, respectively, any variations in environmental conditions that control the two factors can induce a change in Δ.

Internal CO_2 further diffuses to the site of carboxylation inside the chloroplast stroma through intercellular air spaces, through cell wall and plasma membrane, and finally through the liquid phase inside the cell (Flexas et al. 2008). This diffusion component altogether is termed as mesophyll conductance (g_m), and the fractionation factor during internal CO_2 transfer (a_m) is 1.8‰, consisting of a fractionation of CO_2 dissolution (1.1‰, Mook et al. 1974) and a fractionation of liquid phase diffusion (0.7‰, O'Leary 1984). Multiple lines of evidence have indicated that g_m is sufficiently small as to considerably decrease chloroplastic CO_2 concentration (C_c) relative to C_i (Evans et al. 1986; Ogée et al. 2018), thereby limiting photosynthetic rate (Flexas et al. 2008) and affecting Δ (Pons et al. 2009; Ma et al. 2021; Gimeno et al. 2021; Schiestl-Aalto et al. 2021). Theoretical estimations and experimental evidence suggest that the variations in g_m can account for 2 to 8‰ of changes in Δ (Le Roux et al. 2001; Pons et al. 2009; Schiestl-Aalto et al. 2021). Recent studies have revealed that g_m varies with species (Ubierna et al. 2017; Shrestha et al. 2019) and environmental factors, such as temperature (Ubierna et al. 2017; Shrestha et al. 2019) and water stress (Ma et al. 2021; Gimeno et al. 2021).

The most significant discrimination against ^{13}C occurs when CO_2 is utilized by the carboxylating enzymes, such as ribulose 1,5-bisphosphate carboxylase/oxygenase (Rubisco) and phospho*enol*pyruvate carboxylase (PEPc). The two enzymes differ significantly in their discrimination against ^{13}C (Guy et al. 1989): Rubisco discriminates against $^{13}CO_2$ by ca. 30‰, whereas PEPc favors $^{13}CO_2$ by ca. 5.7‰ (Farquhar 1983). Depending on the proportion of PEPc activity, the fractionation factor due to carboxylation (b) can vary between 27 to 30‰ (Pons et al. 2009), with a commonly acknowledged value of ca. 29‰ (Wingate et al. 2007; Busch et al. 2020). Discrimination due to carboxylation depends on the ratio of chloroplastic to ambient CO_2 concentrations (C_c/C_a), and contributes to the largest proportion of overall Δ in most conditions (Busch et al. 2020).

Discrimination between ^{12}C and ^{13}C occurs also in mitochondrial respiration. Due to incomplete knowledge of isotope effects in day respiration metabolism (Tcherkez et al. 2011), to date no agreement on the value of fractionation factor due to day respiration (e) is

reached. While some studies suggested *e* to be ca. 5‰ (Tcherkez et al. 2004; Tcherkez et al. 2010), other studies used an assumed *e* value between -11 and 0‰ (Wingate et al. 2007; Busch et al. 2020; Schiestl-Aalto et al. 2021) or the fractionation factor derived for night respiration (-6‰, Ghashghaie et al. 2003) in isotope discrimination models. Sometimes an apparent fractionation for day respiration (e^*) is incorporated, if $\delta^{13}C$ of respiratory substrates differs from that of new assimilates (Wingate et al. 2007; Tcherkez et al. 2011). Nevertheless, as day respiration is extensively inhibited (Keenan et al. 2019), this uncertainty in *e* often poses insignificant impact on Δ except when day respiration rate (R_d) becomes large relative to net assimilation rate (A_n) (Busch et al. 2020).

During photorespiration, the enzyme catalyzing CO_2 release – glycine decarboxylase – favours the ^{12}C isotope by ca. 20‰ (Tcherkez 2006). This results in ^{13}C-depletion in emitted CO_2 and ^{13}C-enrichment in remaining substrates, which recycle in the photosynthesis process (Wingate et al. 2007). Consequently, photorespiration tends to increase $\delta^{13}C_A$ and lower the value of Δ. Currently, there is no agreement on the value of fractionation factor caused by photorespiration (*f*), which is suggested to be variable among species and with environmental conditions (Ghashghaie et al. 2003), in the range of 8 to 16‰ (Ghashghaie et al. 2003; Igamberdiev et al. 2004; Lanigan et al. 2008; Evans and von Caemmerer 2013; Schubert and Jahren 2018). Overall, photorespiration has a minor effect on Δ, in the order of ca. 1‰ (Igamberdiev et al. 2004; Lanigan et al. 2008; Evans and von Caemmerer 2013), although this effect can be significant at low C_i conditions (Busch et al. 2020).

So far, the fractionation processes associated with g_m dynamics, mitochondrial respiration and photorespiration have not been clearly understood. Advanced knowledge on these processes may be obtained via a thorough comparison of $\delta^{13}C_A$ or Δ derived from IRMS analysis of leaf sugars, online chamber-based $\delta^{13}C$ analysis of CO_2 flux and isotope discrimination models, at high-resolution intra-seasonal scale. Yet, such comparisons are scant in the literature.

1.1.2 Environmental and physiological control on $\delta^{13}C$ of assimilates

The above-mentioned isotope fractionation processes respond sensitively to changes in environmental variables, hence imprinting environmental information in $\delta^{13}C_A$. For instance, temperature has a multifold impact on Δ and $\delta^{13}C_A$. The increase in temperature enhances g_m (Ubierna et al. 2017; Shrestha et al. 2019), resulting in higher Δ values. However, this effect on g_m is counterbalanced by an increase in photorespiration rate with rising temperature, which lowers Δ (Evans and von Caemmerer 2013). Under field conditions, temperature often increases concurrently with photosynthetically active radiation (PAR), together promoting carboxylation rate, reducing the C_i/C_a value and, hence, producing lower Δ and higher $\delta^{13}C_A$ values. High radiation inhibits day respiration and stimulates photorespiration (Wingler et al. 2000; Wehr et al. 2016), both decreasing the magnitude of Δ. Water stress related parameters, such as relative humidity, vapor pressure deficit (VPD) and soil moisture, can also significantly impact the magnitude of Δ. Water stress usually induces a decrease in g_s and g_m (Galiano et al. 2017; Ma et al. 2021; Gimeno et al. 2021), which suppresses the rate of photosynthesis and leads to lower Δ and higher $\delta^{13}C_A$ values.

Central to the physiological control on Δ are stomata, which act as a control valve over the CO_2 diffusion from the atmosphere into leaves. Stomata functioning sufficiently determines the values of C_i/C_a and Δ such that the latter can be described as Eq. 3 in a simplified form (Farquhar et al. 1982).

$$\Delta = a_s + (b - a_s)\cdot C_i/C_a \quad (3)$$

Meanwhile, stomata also control the flux of water vapor out of leaves (E), which has a 1.6 times higher diffusion rate than gaseous CO_2 (Farquhar et al. 1982). The effectiveness of stomatal control can be quantified in terms of intrinsic water use efficiency (iWUE), which is the ratio of A_n to g_s or carbon gains per unit of water loss (Eq. 4; Frank et al. 2015). According to Eq. 4, higher iWUE represents a higher gradient from C_a to C_i, which results in a lower Δ value.

$$\text{iWUE} = A_n/g_s = (C_a - C_i)/1.6 \quad (4)$$

The environmental control on $\delta^{13}C_A$ has been examined by correlation analyses between environmental variables and $\delta^{13}C$ of leaf carbon pools at both diurnal scale (Brandes et al. 2006; Zhang et al. 2019) and intra-seasonal scale (Brendel et al. 2003; Rinne et al. 2015b; Churakova (Sidorova) et al. 2018; 2019). The relationships between climate variables and $\delta^{13}C$ signals have also been studied for annual tree-rings for paleoclimate reconstructions of, for example, temperature (Young et al. 2019), radiation (Helama et al. 2018) and humidity (Liu et al. 2018). Similarly, the relationship between iWUE and Δ (or $\delta^{13}C_A$) (Eqs. 3 and 4) is used for reconstructing iWUE, at both leaf (Stokes et al. 2010; Rumman et al. 2018) and tree-ring levels (Frank et al. 2015; Adams et al. 2020). Such applications are based on the implicit assumption that environmentally or physiologically driven $\delta^{13}C$ signal is passed from leaf assimilates to leaf or tree-ring biomass with limited distortion. However, this assumption is not always valid.

1.2 Modification of $\delta^{13}C$ signal in post-photosynthetic processes

$\delta^{13}C$ of tree biomass or respired CO_2 often differs from $\delta^{13}C_A$, because of further modification of isotopic signatures along the pathway from fresh assimilates towards the end products. This post-photosynthetic modification of $\delta^{13}C$ includes, but is not limited to, possible fractionation occurring during enzyme-catalyzed conversion of metabolites, fractionation during sugar export and import, fractionation during dark respiration, use of reserves, and temporal and spatial integration of $\delta^{13}C$ signal.

1.2.1 Fractionation during conversion of metabolites

Isotope fractionation occurs during the conversion or formation of metabolites, which leads to different $\delta^{13}C$ signals between organic compounds (Figure 2). One of the most intriguing examples is the $\delta^{13}C$ offset between the two main photosynthates, sucrose and starch. This $\delta^{13}C$ offset is mainly caused by an equilibrium of chloroplast aldolase reaction under high photosynthesis rate, when ^{13}C-enriched triose-phosphates (the initial product of photosynthesis) are preferentially condensed to form fructose-1,6-bisphosphates and subsequently starch in the chloroplast (Gleixner and Schmidt 1997; Gleixner et al. 1998). As a result, the ^{13}C-depleted triose-phosphates are exported to the cytosol to form sucrose. $\delta^{13}C$ offset may also exist between sucrose and hexoses (glucose and fructose), often with a higher $\delta^{13}C$ value observed in sucrose. This $\delta^{13}C$ offset is probably linked with the fractionation against ^{13}C during invertase activity, which catalyzes the conversion of sucrose to hexoses

(Mauve et al. 2009). Compared with sugars, pinitol, one of the most abundant sugar alcohols in trees, is more ^{13}C-depleted. As pinitol and sugars are the main components of water-soluble carbohydrates (WSCs) (Rinne et al. 2015b; Churakova (Sidorova) et al. 2019), a lower $\delta^{13}C$ value is expected in WSCs compared with sugars. Similarly, $\delta^{13}C$ value of total water-soluble organic matter (WSOM) tends to be lower than that of sugars, but it varies considerably due to the contribution of other components. Whereas cellulose, the major component of total organic matter (TOM), may have higher $\delta^{13}C$ value compared with sucrose (Rinne-Garmston et al. unpublished), the presence of ^{13}C-depleted lipids and lignin results in a lower $\delta^{13}C$ value in TOM relative to sucrose.

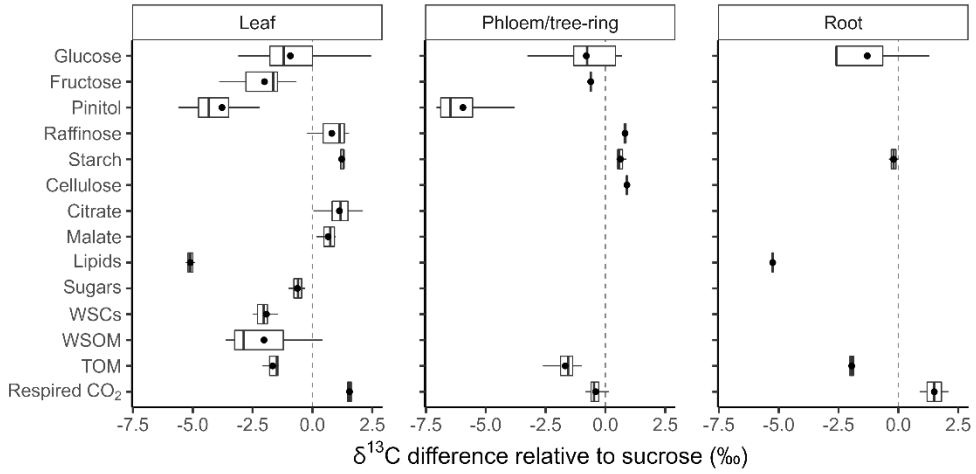

Figure 2. Comparison of $\delta^{13}C$ in different tree carbon pools and respired CO_2, expressed relative to sucrose. The box encompasses the interquartile range of the data, the line represents the median, the dot represents the mean, the tails extend to 1.5 times of the interquartile range. The vertical dashed line is included for easy reference to sucrose $\delta^{13}C$. WSCs is water-soluble carbohydrates, WSOM is water-soluble organic matter, and TOM is total organic matter. References used for each category are listed in Table 1.

Table 1. References used for each category in Figure 2.

Category	Leaf	Phloem/tree-ring	Root
Glucose	Damesin and Lelarge 2003; Sun et al. 2012; Rinne et al. 2015b; Smith et al. 2016; Churakova (Sidorova) 2018; 2019; Bögelein et al. 2019; Rinne-Garmston et al. unpublished	Damesin and Lelarge 2003; Smith et al. 2016; Rinne-Garmston et al. unpublished	Sun et al. 2012; Rinne-Garmston et al. unpublished
Fructose	Damesin and Lelarge 2003; Rinne et al. 2015b; Smith et al. 2016; Churakova (Sidorova) et al. 2018; 2019; Bögelein et al. 2019	Damesin and Lelarge 2003; Maunoury et al. 2007	
Pinitol	Rinne et al. 2015b; Smith et al. 2016; Churakova (Sidorova) et al. 2018; 2019; Bögelein et al. 2019	Smith et al. 2016	
Raffinose	Merchant et al. 2011	Merchant et al. 2011	
Starch	Damesin and Lelarge 2003; Sun et al. 2012	Damesin and Lelarge 2003; Vincent-Barbaroux et al. 2019	Sun et al. 2012
Cellulose		Rinne-Garmston et al. unpublished	
Citrate	Churakova (Sidorova) et al. 2018; 2019		
Malate	Churakova (Sidorova) et al. 2018; 2019		
Lipids	Sun et al. 2012		Sun et al. 2012
Sugars	Bögelein et al. 2019		
WSCs	Rinne et al. 2015b; Churakova (Sidorova) et al. 2018; 2019; Rinne-Garmston et al. unpublished		
WSOM	Merchant et al. 2011		
TOM	Damesin and Lelarge 2003; Sun et al. 2012	Damesin and Lelarge 2003; Maunoury et al. 2007; Vincent-Barbaroux et al. 2019	Sun et al. 2012
Respired CO_2	Sun et al. 2012	Damesin and Lelarge 2003; Maunoury et al. 2007; Vincent-Barbaroux et al. 2019	Sun et al. 2012

1.2.2 Fractionation during sugar export and import

It has been long speculated that carbon isotope fractionation may occur in the export and import of sugars during phloem transport (Damesin and Lelarge 2003; Ghashghaie et al. 2003; Badeck et al. 2005; Bögelein et al. 2019). Three potential mechanisms may be involved. First, given that sucrose is the predominant transport sugar in trees (Rennie and Turgeon 2009; Julius et al. 2017), fractionations are assumed to occur at the loading site associated with plasma-membrane sucrose transporters (Xu et al. 2020), or at the unloading site during sucrose cleavage to hexoses via invertase (Gilbert et al. 2012). The former assumption has not been proved by experimental evidence (Gilbert et al. 2012). However, the fractionation against ^{13}C during invertase activity (Mauve et al. 2009) may lead to ^{13}C-depeletion in the imported hexoses in relation to the transport sugar – sucrose. Second, the sugar transport pool in the exporting leaf cell may have a different $\delta^{13}C$ signal compared with the overall sugar pool within the cell. Brauner et al. (2014) suggested a fast transport pool of sucrose in cytosol and a slow one in the vacuole. Thereby, a higher $\delta^{13}C$ value in the cytosol pool may lead to ^{13}C-enrichment in phloem sugars relative to leaf assimilates (Bögelein et al. 2019). Alternatively, Hobbie and Werner (2004) suggested that the preferential use of ^{12}C for the formation of lipids and lignin led to ^{13}C-enrichment of the remaining leaf assimilates, including the transport sugar pool. Third, the accumulation and remobilization of transitory starch govern the diel rhythm of $\delta^{13}C$ in exported sugars from leaves, which may lead to an overall ^{13}C-enrichment in exported sugars compared with the primary assimilates (Gessler et al. 2008; Gessler and Ferrio 2022).

1.2.3 Fractionation during dark respiration

Enrichment of ^{13}C in leaf or shoot respired CO_2 relative to putative respiratory substrates has been commonly reported for various tree species (Hymus et al. 2005; Sun et al. 2012; Figure 2) and non-woody plant species (Klumpp et al. 2005; Bathellier et al. 2008). Three main hypotheses have been proposed to explain the ^{13}C-enrichment of respired CO_2 in the autotrophic tissues. First, CO_2 is preferentially released from the ^{13}C-enriched C-3 and C-4 positions of glucose (Rossmann et al. 1991; Gilbert et al. 2012) via incomplete oxidation of pyruvate (Ghashghaie et al. 2003; Bathellier et al. 2008). In other words, C-1 of pyruvate (from C-3 and C-4 of glucose) is decarboxylated via pyruvate dehydrogenase while the lighter carbon atoms (C-1, C-2, C-5 and C-6 of glucose) are not fully decarboxylated in the Krebs cycle. Second, leaf respiration at dark is fueled by carbohydrates derived from transient starch (Sun et al. 2012), which is relatively ^{13}C-enriched compared with the initial product of photosynthesis, triose phosphate (Gleixner et al. 1998). Third, ^{13}C-enriched metabolites that accumulate during the light period, such as malate, are used as respiratory substrate during the post-illumination respiration period (Barbour et al. 2007; Gessler et al. 2009a), which may be superimposed on the ^{13}C-enrichment in leaf dark-respired CO_2 (Werner et al. 2009).

Both higher (Damesin and Lelarge 2003; Brandes et al. 2006; Gessler et al. 2007; Maunoury et al. 2007; Kodama et al. 2008; Sun et al. 2012; Wingate et al. 2010) and lower (Maunoury et al. 2007; Wingate et al. 2010) $\delta^{13}C$ values in stem or root respired CO_2 relative to biomass or putative substrates have been reported for various tree species. By contrast, for non-woody species, respired CO_2 has been found to be consistently ^{13}C-depleted in respect to putative substrates in roots (Badeck et al. 2005; Klumpp et al. 2005; Bathellier et al. 2008; Gessler et al. 2009a) and stem (Badeck et al. 2005; Gessler et al. 2009a). These contrasting results likely arise from the following reasons. First, different substrates have been analyzed

for $\delta^{13}C$ in different studies. For example, TOM in Damesin and Lelarge (2003), Brandes et al. (2006) and Maunoury et al. (2007), WSOM in Gessler et al. (2007) and Wingate et al. (2010), total soluble sugars in Maunoury et al. (2007), and individual sugars in Damesin and Lelarge (2003), Maunoury et al. (2007) and Sun et al. (2012). Varying $\delta^{13}C$ signals of different substrates (Figure 2) may result in a discrepancy in the sign of respiratory isotope fractionation. Second, the direction of respiratory isotope fractionation is likely to be species-specific (Sun et al. 2012; Priault et al. 2009), due to the difference in carbon allocation between respiratory pathways (Priault et al. 2009). Slow-growing species (such as evergreen trees) tend to maintain high carbon flux through pyruvate dehydrogenase activity combined with a consistently low Krebs cycle activity, thus resulting in ^{13}C-enrichment in respired CO_2. In comparison, fast-growing species (such as deciduous trees, herbs or grasses) with high respiration demand require full oxidation of the substrates (Priault et al. 2009). Third, a shift in the respiratory substrates over the growing season, for example, from recently fixed assimilates to reserves, may change the direction of respiratory isotope fractionation (Maunoury et al. 2007). In that sense, the results are dependent on the timing of measurements. Fourth, the ^{13}C-depletion of respired CO_2 from roots and stem for non-tree species may be related to intensive activities of oxidative pentose phosphate (Bathellier et al. 2008) and PEPc (Gessler et al. 2009a). The former decarboxylates the ^{13}C-depleted C-1 position of glucose (Rossmann et al. 1991), whereas the latter refixes CO_2 with a net fractionation favoring ^{13}C by 5.7‰ (Farquhar 1983), thus enriching the product and depleting the remaining CO_2.

1.2.4 Use of reserves

Use of reserves for biomass growth or respiration can also deviate $\delta^{13}C$ of tree biomass or respired CO_2 from $\delta^{13}C_A$, as reserves often have a different $\delta^{13}C$ value than fresh assimilates. The use of reserves for supporting leaf flush (Kagawa et al. 2006; Gaudinski et al. 2009; February and Higgins 2016), earlywood formation (Jäggi et al. 2002; McCarroll et al. 2017; Vincent-Barbaroux et al. 2019) or root growth (Gaudinski et al. 2009; Villar-Salvador et al. 2015) has been reported for various deciduous trees and some evergreen species under field conditions. In addition, reserves may be used for the growth of reaction wood (Guérard et al. 2007) or respiration of stem (Muhr et al. 2018) and roots (Hartmann et al. 2013; Aubrey and Teskey 2018) under stress conditions. Most often, the major carbon reserve pool, starch (Hartmann and Trumbore 2016), is utilized, enriching ^{13}C in biomass or respired CO_2. In other cases, lipids and proteins can also feed respiration under severe stress (Hartmann et al. 2013; Fischer et al. 2015; Hanf et al. 2015), which may result in ^{13}C-depletion of respired CO_2.

1.2.5 Temporal and spatial integration of $\delta^{13}C$ signal

$\delta^{13}C$ of tissue biomass or respired CO_2 reflects a time-integrated signal, and therefore may differ from $\delta^{13}C_A$, which changes rapidly in response to environmental factors. Initially, a short-term carry-over effect exists in both leaf (Desalme et al. 2017) and phloem (Keitel et al. 2003) sugar pools, which provide the substrate for biomass growth or respiration. Next, tissue biomass is formed over a period, when the $\delta^{13}C$ signal of the substrate is integrated.

Spatial integration of phloem sugars, that is, the mixing of sugars assimilated at different canopy gradients, also contributes to the post-photosynthetic alteration of $\delta^{13}C$ signal. Due to light gradient, $\delta^{13}C_A$ at the lower canopy can be up to 8‰ lower than that at the upper

canopy (Schleser 1990; Le Roux et al. 2001; Bögelein et al. 2019). Thereby, a higher contribution of assimilates from the lower canopy to phloem sugars tends to lower the $\delta^{13}C$ of trunk phloem sugars. Nevertheless, the degree of vertical mixing patterns of assimilates in phloem is likely species-specific. Bögelein et al. (2019) reported a major contribution of assimilates from the upper crown to the phloem sugar pool at breast height for *Fagus sylvatica*, but not for *Pseudotsuga menziesii*. Likewise, Li and Zhu (2011) demonstrated that lower canopy leaves could provide a surplus of assimilates to the base trunk for *Pinus koraiensis*, but not for *Larix gmelinii*.

To date, significant gaps still exist in our knowledge about how the environmentally driven $\delta^{13}C$ signal in leaf assimilates is modified by these post-photosynthetic processes prior to tree-ring formation (Gessler et al. 2014). These knowledge gaps hinder a reliable interpretation of tree-ring $\delta^{13}C$ data in retrospect for environmental studies.

1.3 New stable isotope analysis tools

Future progress in understanding the preservation of $\delta^{13}C$ signal in trees and using tree-ring $\delta^{13}C$ for backtracking environmental and physiological information relies on improvements in two areas. First, compound-specific $\delta^{13}C$ analysis of leaf sugars at high-resolution intra-seasonal scale in combination with isotope discrimination models can improve our understanding of photosynthetic isotope fractionation. Second, concurrent high-resolution intra-seasonal $\delta^{13}C$ analysis of tree-rings can not only help decipher post-photosynthetic isotope fractionation processes but also reconstruct environmental and physiological information at a finer scale, beyond the conventionally used annual scale (Rinne-Garmston et al. 2022).

1.3.1 Compound-specific $\delta^{13}C$ analysis

Compound-specific isotope analysis (CSIA) for $\delta^{13}C$ was introduced by Barrie et al. (1984) via coupling online gas chromatography to an IRMS. Nevertheless, this method requires substantial derivatization of analyzed materials, such as carbohydrates, and the corrections needed for the carbon atoms added during derivatization largely affect the accuracy of $\delta^{13}C$ results (Boschker et al. 2008). Later, high-performance liquid chromatography (HPLC) separation of sugar extracts and off-line isotope analysis became a common practice for determining $\delta^{13}C$ of an individual sugar (Duranceau et al. 1999; Damesin and Lelarge 2003; Maunoury et al. 2007; Sun et al. 2012; Vincent-Barbaroux et al. 2019). This method, however, requires a substantial amount of sugar extracts. In addition, it is labor-intensive and challenging due to the close co-elution of individual sugars from an analytical column. Recent advances in online coupling of HPLC via an interface to an IRMS (hereafter HPLC-IRMS, Krummen et al. 2004) have significantly improved the ease in sugar separation and reduced the sample size needed for isotope determination. Moreover, examination of optimal chromatographic conditions for HPLC-IRMS analysis as well as sample preparation protocols provides an example of standardized procedures for compound-specific $\delta^{13}C$ analysis of leaf sugar extracts (Rinne et al. 2012).

Currently, compound-specific $\delta^{13}C$ analysis at natural abundance has been applied to a limited number of studies on tree species to examine (1) $\delta^{13}C$ differences between individual compounds and biomass or respired CO_2 (Damesin and Lelarge 2003; Maunoury et al. 2007; Sun et al. 2012; Rinne et al. 2015a; Vincent-Barbaroux et al. 2019); (2) leaf-to-phloem carbon

isotope fractionation (Merchant et al. 2011; Smith et al. 2016; Bögelein et al. 2019); (3) environmental drivers on $\delta^{13}C$ of individual compounds in leaves (Rinne et al. 2015b; Churakova (Sidorova) et al. 2018; 2019). Their findings illustrate that environmental and physiological signals derived from $\delta^{13}C$ of bulk matter may be dampened (but see Smith et al. 2016), and that CSIA confers a significant improvement in understanding the recording and modifying of $\delta^{13}C$ signatures in trees. In addition, CSIA has also been combined with $^{13}CO_2$ pulse-labelling technique, to explore carbon allocation patterns in trees upon changes in environmental conditions, such as elevated CO_2 and soil warming (Streit et al. 2012) or drought (Galiano et al. 2017).

1.3.2 Intra-seasonal tree-ring $\delta^{13}C$ analysis

Traditionally, intra-seasonal tree-ring $\delta^{13}C$ analysis can be achieved by cutting annual rings to micro-sections via a microtome (Kagawa 2003; Helle and Schleser 2004; Zeng et al. 2017). This manual preparation process is labor-intensive, and not suitable for narrow rings (Zeng et al. 2017) due to restrictions on sample amount needed for IRMS analysis. The ease of determining high-resolution intra-seasonal $\delta^{13}C$ of tree-rings has later been greatly improved with the introduction of an online method, which combines laser ablation (LA), combustion, gas chromatography and IRMS (hereafter LA-IRMS, Schulze et al. 2004). LA-IRMS has increased the spatial resolution for $\delta^{13}C$ analysis down to 40 µm with high accuracy (Schulze et al. 2004). In addition, as this approach requires relatively small quantities of samples, it is considered as less invasive and virtually non-destructive in comparison with the manual method (Loader et al. 2017).

LA-IRMS has been applied to studies on a variety of tree species to examine the intra-ring $\delta^{13}C$ patterns, often with the combination of other tree-ring proxies, such as wood density (Skomarkova et al. 2006) and wood anatomical traits (Vaganov et al. 2009; Battipaglia et al. 2010; De Micco et al. 2012; Fonti et al. 2018). Sometimes, the timing of intra-seasonal tree-ring $\delta^{13}C$ measurements has been estimated via xylogenesis observations (Rinne et al. 2015a; Fonti et al. 2018) or wood growth modelling (Soudant et al. 2016), allowing their comparison with environmental variables (Soudant et al. 2016; Fonti et al. 2018) and leaf sugar $\delta^{13}C$ signals (Rinne et al. 2015a) on the temporal scale. These studies have not only revealed the influence of environmental variables (Soudant et al. 2016), tree growth rate (Vaganov et al. 2009), tree age (Fonti et al. 2018), stand structure (Skomarkova et al. 2006) and the degree of reserve use (Skomarkova et al. 2006; Vaganov et al. 2009; Bryukhanova et al. 2011; Rinne et al. 2015a; Fonti et al. 2018) on the intra-seasonal tree-ring $\delta^{13}C$ profiles, but also shed light on the post-photosynthetic processes via concurrent CSIA conducted on leaf sugars (Rinne et al. 2015a).

There is no doubt that the combination of CSIA and LA-IRMS for tree $\delta^{13}C$ studies can further broaden our understanding of $\delta^{13}C$ dynamics in different tree compartments and provide us great insights on tree's response to environmental change.

2. MOTIVATION, OBJECTIVES AND HYPOTHESES

Tree $\delta^{13}C$ is a powerful tool to study the response of trees to environmental change. The interpretation of tree $\delta^{13}C$ signal relies on in-depth knowledge of how $\delta^{13}C$ is recorded and modified in trees during photosynthetic and post-photosynthetic processes. Some aspects of the two processes, however, remain poorly understood. For instance, how do $\delta^{13}C_A$ estimates from the three methods, that is, IRMS analysis of leaf carbon pools, online chamber-based $\delta^{13}C$ analysis of CO_2 flux and isotope discrimination models, compare with each other at intra-seasonal scale, and what mechanisms are responsible for their offsets if there are any? To what extent and by what mechanisms is the $\delta^{13}C$ signal altered from leaf assimilates to leaf carbon pools, tree-rings and respired CO_2? And how does this post-photosynthetic $\delta^{13}C$ alteration impact the interpretation of environmental and physiological signals retrieved from leaf and tree-ring $\delta^{13}C$?

The objectives of this thesis are to quantify the earlier unknown parts of photosynthetic and post-photosynthetic isotope fractionation processes and, with the gained information, to interpret the environmental and physiological signals derived from tree $\delta^{13}C$, via a case study on Scots pine (*Pinus sylvestris* L.) in two boreal forests. The specific objectives are to:

(1) interpret leaf-level $\delta^{13}C$ signal via comparing $\delta^{13}C_A$ estimates from IRMS analysis of leaf carbon pools, online chamber-based $\delta^{13}C$ analysis of CO_2 flux and isotope discrimination models at intra-seasonal scale (studies I and II);
(2) quantify the $\delta^{13}C$ offsets between different carbon pools in different tree tissues, and understand the role of post-photosynthetic isotope fractionation and use of reserves in determining these $\delta^{13}C$ offsets (studies I, III and IV);
(3) retrieve environmental and physiological information from leaf-level $\delta^{13}C$ signal, and examine the suitability of LA-IRMS-derived tree-ring $\delta^{13}C$ data for intra-seasonal iWUE estimation (studies I and IV).

Correspondingly, the specific hypotheses of this thesis are:

(1) Differences between leaf sugar $\delta^{13}C$, chamber-based $\delta^{13}C_A$ and modelled $\delta^{13}C_A$ can be reconciled by g_m dynamics and carry-over effects of leaf sugars (studies I and II).
(2) CSIA provides more accurate knowledge of post-photosynthetic fractionation processes than bulk isotope analysis, and there is no clear use of reserves for biomass growth of the studied trees (studies I, III and IV).
(3) CSIA data better record environmental and physiological signals than bulk isotope data at leaf level (study I), and tree-ring $\delta^{13}C$ is suitable for tracing intra-seasonal iWUE variability (study IV).

3. MATERIALS AND METHODS

A detailed description of the materials and methods can be found in the manuscripts attached at the end of the dissertation (studies I–IV).

3.1 Site description

The study was conducted at two ~60-year-old Scots pine dominated boreal forest sites in Finland: Värriö (SMEAR I, Station for Measuring forest Ecosystem-Atmosphere Relations) and Hyytiälä (SMEAR II). Locations of the sampling sites are illustrated in Figure 3.

Värriö (67°46′N, 29°35′E, 400 m a.s.l.) is situated at the arctic-alpine timberline in northern Finland. The stand density in Värriö is ca. 750 ha^{-1} with the mean height of the trees being 10 m (Kulmala et al. 2019). The soil in Värriö is classified as a haplic podzol with sand tills in FAO classification (FAO–UNESCO 1990), with a 0–2.2 cm top layer (F-horizon), a 0–1.2 cm humus layer (H-horizon), a 1–4.5 cm eluvial horizon (A-horizon) and a 1–6 cm illuvial horizon (B-horizon) (Köster et al. 2014). In Värriö, the mean annual temperature was 0.1°C, but mean monthly temperature varied from -10.8°C in January to 13.6°C in July. The mean annual precipitation in Värriö was 607 mm, with 36% distributed during June to August (from 1991 to 2020, Jokinen et al. 2021). Growing season in Värriö lasts for ca. 114 d (Köster et al. 2015).

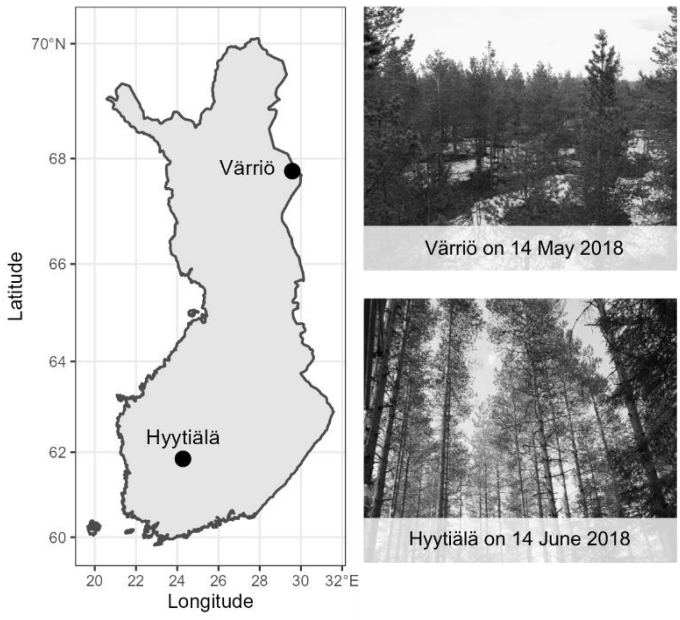

Figure 3. Locations and photographs of the study sites.

Hyytiälä (61°51′N, 24°17′E, 170 m a.s.l.) is located in southern Finland. The stand is mixed with Norway spruce (*Picea abies* (L.) Karst) and birch (*Betula pubescens* Ehrh. and *Betula pendula* Roth) in the understory. The stand density in Hyytiälä for trees with diameter >5 cm at 1.3 m height was 1304 ha^{-1}, and the dominant tree height was 23.5 m in year 2018 (Kolari et al. 2022). The soil is a haplic podzol on glacial till (FAO–UNESCO 1990), with an organic layer depth of 5.4 cm (Kulmala et al. 2008) and a mineral soil layer depth of 0.5 to 0.7 m over the bedrock (Schiestl-Aalto et al. 2019). During 1991 to 2020, the mean annual temperature was 4.1°C, but mean monthly temperature varied from -6.7°C in February to 16.2°C in July. During this period, the mean annual precipitation was 690 mm, with 34% falling between June and August (Jokinen et al. 2021). The growing season in Hyytiälä is ca. 150 d (Danielewska et al. 2015).

Environmental data for the study sites were obtained from the AVAA Smart SMEAR portal (https://smear.avaa.csc.fi/).

3.2 Sampling

Needles, stem phloem, roots and tree-rings were collected for isotope analysis, and micro-cores for xylogenesis observation.

In 2018 and 2019, one-year-old and current-year needles were collected separately 20 times from five mature trees per site and season. Needles were harvested between 13:00 to 16:00 h (UTC+2) at sun-exposed positions 2 m below the top of the canopy, using a walk-in scaffolding tower and a 10 m long branch scissor or via tree-attached ladders. The sampling started before the start of radial growth (early May in Hyytiälä and late May in Värriö) and ended after the cessation of radial growth (October in both sites), with relatively higher sampling frequency at the beginning of the growing season. For each needle sampling day, micro-cores (diameter 2 mm, length 15 mm) at 1.3 m height were also collected from five mature trees using Trephor corer (Costruzioni Meccaniche Carabin C., Belluno, Italy) (Rossi et al. 2006). Phloem samples at 1.3 m height were collected from five mature trees with a 2 cm diameter corer six times per site and year. In Hyytiälä, fine roots (< 2 mm) at 5–15 cm depth were excavated 11 times during May to October in 2018, from three random spots ca. 100 m away from the sampling trees to prevent disturbance on the study site. All needle, phloem and root samples were micro-waved within 2 h after collection at 600 W for 1 min to stop enzymatic and metabolic activities (Wanek et al. 2001). Samples were then dried and homogenized into fine powder. After the cessation of growth in 2019, one tree-ring core or cross section was collected at breast height from five mature trees per site.

All the sampling trees at each site were in the same vicinity, of the same size and with the same growth conditions. Trees sampled for tree-rings, phloem and micro-cores were not entirely the same as that for needles, in order to minimize the damage to the trees under long-term monitoring. Nevertheless, the average values and trends of $\delta^{13}C$ from five trees should accurately represent the situation of the study sites (Leavitt and Long 1984).

3.3 $\delta^{13}C$ and concentration analysis

3.3.1 Extraction and purification of WSCs

Extraction and purification of WSCs were performed according to Wanek et al. (2001) and Rinne et al. (2012), respectively. In brief, ca. 60 mg of needle, phloem or root powders were transferred into a 2 ml reaction vial and re-suspended in 1.5 ml of deionized water. The vials were placed in a water bath at 85°C for 30 min, cooled for 30 min, and centrifuged at 10 000 g for 2 min. The separated supernatant was then purified by three types of sample preparation cartridges (Dionex OnGuard II H, A & P cartridges, Thermo Fisher Scientific) to remove amino acids, organic acids and phenolic compounds. The purified samples were subsequently freeze-dried, dissolved in 1 ml deionized water, filtered through a 0.45 µm syringe filter, and stored at -20°C until isotope analysis.

3.3.2 Extraction of starch

Starch was extracted from the pellet of the hot water extraction by enzymatic hydrolysis (Wanek et al. 2001; Lehmann et al. 2019). The pellet in each reaction vial was washed with 1.2 ml methanol/chloroform/water (12:5:3, v/v/v) solution four times and with 1.2 ml deionized water three times to remove lipids. Lipid-free pellet in each vial was re-suspended in 0.75 ml deionized water and boiled at 99°C for 15 min in a water bath to gelatinize starch. Starch in pellet was then hydrolyzed at 85°C in a water bath for 2 h after adding 0.25 ml purified (by Vivaspin 15R, Sartorius, Göttingen, Germany) α-amylase (EC 3.2.1.1, Sigma-Aldrich) solution of 3000 U mL^{-1}. The hydrolyzed starch was later separated from enzymatic residues with centrifugation filters (Vivaspin 500, Sartorius, Göttingen, Germany) and stored at -20°C until isotope analysis.

3.3.3 Bulk $\delta^{13}C$ analysis

$\delta^{13}C$ values of WSCs, starch and TOM were measured at the Stable Isotope Laboratory of Luke (SILL, Natural Resources Institute Finland), using an elemental analyzer (EA) (Europa EA-GSL, Sercon Limited, Crewe, UK) coupled to an IRMS (20-22 IRMS, Sercon Limited, Crewe, UK). Aliquots of purified WSCs and hydrolyzed starch were pipetted into tin capsules (5×9 mm, Säntis, Teufen, Switzerland), freeze-dried and wrapped, while needle powder was weighed directly into tin capsules. The $\delta^{13}C$ results were calibrated against IAEA-CH3 (cellulose, -24.724‰), IAEA-CH7 (polyethylene, -32.151‰) and an in-house sucrose reference (Sigma Aldrich, -12.22‰). Measurement precision determined from multiple analysis of quality control materials was 0.1‰ (SD).

3.3.4 Compound-specific $\delta^{13}C$ analysis

CSIA for $\delta^{13}C$ of WSCs was done at the Stable Isotope Research Laboratory of WSL (Birmensdorf, Switzerland) using a HPLC-IRMS with a Thermo LC Isolink interface (Krummen et al. 2004). Four sugars or sugar alcohols with the concentration of from 20 to 180 ng carbon μl^{-1} were detected: sucrose, glucose, fructose and pinitol/myo-inositol. As pinitol and myo-inositol co-elute from the analytical column and the two compounds have close relation in biosynthetic pathways and in stress-related processes (Rinne et al. 2012), they were treated as one compound (referred to as “pinitol” hereafter). Compound-matched

external standard solutions with EA-IRMS determined $\delta^{13}C$ values were analyzed every ten samples to correct the $\delta^{13}C$ results by HPLC-IRMS. The measurement precision (SD) of pinitol, sucrose, glucose and fructose standards were 0.23‰, 0.24%, 0.30% and 0.59%, respectively.

3.3.5 Concentration determination

Compound-specific concentrations of WSCs were determined by the concentration and peak area linearity of the standards in HLPC-IRMS analysis (Rinne et al. 2012). Concentrations of WSCs were determined as the sum of concentrations of the four detected compounds (study I), or based on the weights of WSCs in tin capsules and the weights of plant materials used for extraction (studies II and III). Concentration determination of starch was based on the weight of hydrolyzed starch pipetted into the tin capsules, the sample mass used for starch extraction and a conversion factor accounting for the hydrolysis efficiency of starch to glucose (study I).

3.3.6 Intra-seasonal $\delta^{13}C$ analysis of tree-rings

Tree-ring samples were air dried and gently surfaced using sandpaper to facilitate ring identification. Each sample was then placed in distilled water in an ultrasonic bath for 30 min to remove the sawdust. Annual tree-rings from 2002 to 2019 were then carefully identified via statistical crossdating (WinDENDRO™). Mobile resin and extractives of the samples were removed using a 2:1 toluene-ethanol mixture in a Soxhlet extractor for 48 h (Loader et al. 1997). Residual toluene and ethanol in the samples were removed by bathing the samples with distilled water in the Soxhlet extractor and then by air drying. Resin-extracted tree-ring was directly used in LA-IRMS analysis, as suggested in Schulze et al. (2004).

Intra-seasonal $\delta^{13}C$ series of tree-rings formed during 2002 to 2019 in both sites were analyzed via LA-IRMS at the SILL (study IV), following the operation principle in Schulze et al. (2004) and Loader et al. (2017). Depending on the ring width, from 5 to 33 laser tracks of 40 μm width were ablated per tree-ring for $\delta^{13}C$ analysis. The $\delta^{13}C$ results were calibrated against USGS-55 (Mexican ziricote tree powder, -27.13‰) and an in-house reference (yucca tree powder, -15.46‰), both of which were hydraulic-pressed into 10 mm disks. IAEA-C3 cellulose paper was measured concurrently for quality control. The LA-IRMS measured $\delta^{13}C$ value of IAEA-C3 (-24.69±0.24‰) is in line with the certified value (-24.91±0.49‰).

3.4 Yearly tree-ring growth

Yearly tree-ring growth curve for each site was monitored by two methods: xylogenesis observations for years from 2007 to 2009 and from 2018 to 2019 (Jyske et al. 2014), and a dynamic growth model *Carbon Allocation Sink Source Interaction* (CASSIA, Schiestl-Aalto et al. 2015) for years from 2002 to 2019.

For xylogenesis observations, micro-core sections were prepared and analyzed according to Jyske et al. (2014) to determine the number of current-year tracheids in the enlargement, wall-thickening and lignification, and mature phases. The growth curves for tracheid production and tracheid maturation were obtained via Gompertz fitting (Zeide 1993) on the number of total and mature current-year tracheids, respectively. Meanwhile, the dimensional growth curve of tracheid production and the number-based growth curve of tracheid

maturation were modelled with CASSIA using input parameters validated for Hyytiälä and Värriö (Schiestl-Aalto et al. 2015; 2019). The number-based growth curves were then transferred to dimensional growth curves, using a non-linear fitting curve between cell number and tree-ring width (study IV). The results of the two methods were compared, and the uncertainty of CASSIA results was discussed in study IV.

With known growth curves and relative position of each LA-IRMS measurement within a tree-ring, the growth period for each LA-IRMS measurement was determined (Figure 4). This information was used for timing intra-seasonal tree-ring $\delta^{13}C$ and iWUE derived therefrom (study IV).

3.5 Gas exchange measurements

Automated chamber systems were implemented for measuring CO_2 fluxes from shoot, stem and soil (Figure 5). For years from 2002 to 2019, transparent acrylic plastic chambers were installed at the top canopy of one to four mature trees for both sites. Each chamber enclosed a debudded one- or two-year-old shoot (Altimir et al. 2002; Kolari et al. 2009). Different types of shoot chambers were employed over the years in Hyytiälä, whereas the chamber design remained the same (Version 1 in Figure 5) in Värriö. In 2018, a custom-made stem chamber was built around the stem at 15 m height of one mature tree in Hyytiälä (Rissanen et al. 2020). Nearby this tree, a transparent soil chamber of 40 × 80 × 25 cm was placed with all ground vegetation removed (Aaltonen et al. 2013).

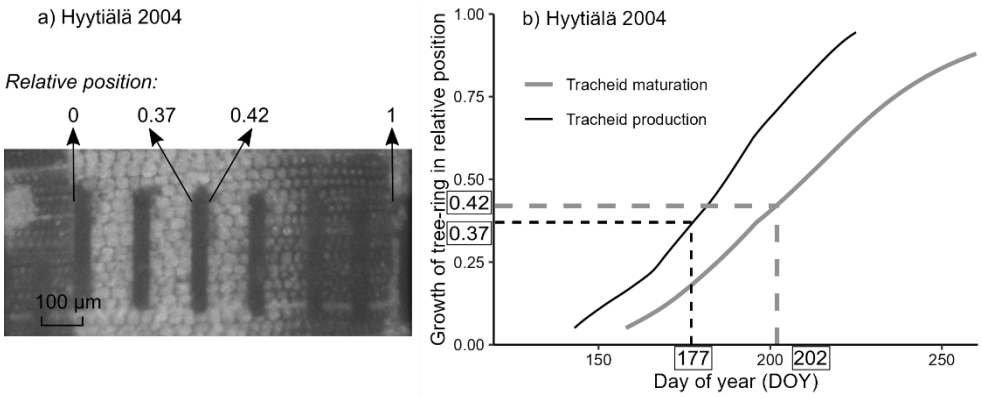

Figure 4. Example of how the formation period of an LA-IRMS measurement was defined. (a) Relative positions of an LA-IRMS measurement within a tree-ring; (b) formation period of the LA-IRMS measurement based on the growth curves of tracheid production and maturation for the specific year and site.

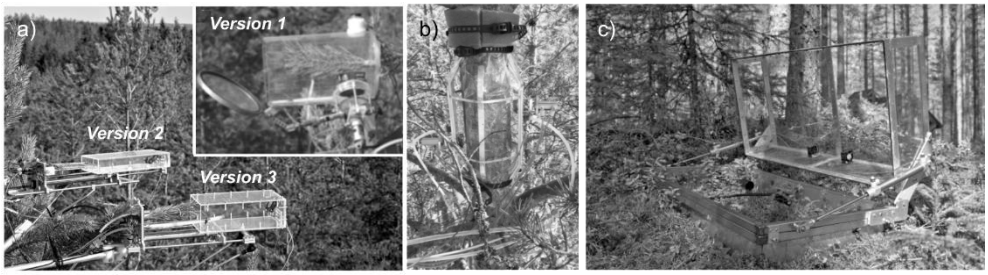

Figure 5. The gas exchange measurement chambers used in this study. (a) Automated shoot chambers (photo by Juho Aalto; Kolari et al. 2012); (b) Custom-made stem chamber (Rissanen et al. 2020); (c) Automated soil chamber (the same type but without vegetation inside, photo by Juho Aalto).

The automatic chambers were intermittently closed one by one from 50 to 180 times a day, with sample air drawn to gas analyzers (URAS-4, Hartmann & Braun, Germany; G2201-I, Picarro, USA and LI-840, LiCor, USA). Based on instantaneous CO_2 and H_2O concentrations during chamber closure, CO_2 fluxes and H_2O fluxes were calculated (Kolari et al. 2012). Flux data with high relative humidity (over 75% or 85%) were omitted to avoid unreliable measurements due to condensation of water droplets (Altimir et al. 2006). Small fluxes (A_n < 0.5 μmol m^{-2} s^{-1} and E < 0.1 mmol m^{-2} s^{-1}) were discarded from further analysis given the uncertainties in the calculation of small fluxes. In 2018, the $\delta^{13}C$ of CO_2 fluxes was determined from the ratio of $^{13}CO_2$ flux to $^{12}CO_2$ flux with Picarro G2201-I. The $\delta^{13}C$ values of CO_2 were calibrated by reference CO_2 gases (Air Liquide, Houston, USA) with $\delta^{13}C$ of -19.0‰ and -3.1‰.

3.6 Isotope discrimination models

Photosynthetic carbon isotope discrimination in Hyytiälä during the growing season of 2018 was estimated by two approaches: a classical one in study I (Eq. 5; Farquhar et al. 1982) and a revised version following Wingate et al. (2007) in study II (Eq. 6).

$$\Delta = a_s \frac{C_a - C_i}{C_a} + a_m \frac{C_i - C_c}{C_a} + b\frac{C_c}{C_a} - f\frac{\Gamma_*}{C_a} - e\frac{R_d}{kC_a}, \quad (5)$$

$$\Delta = \frac{kC_a}{kC_a - R_d}\{a_b \frac{C_a - C_s}{C_a} + a_s \frac{C_s - C_i}{C_a} + a_m \frac{C_i - C_c}{C_a} + b\frac{C_c}{C_a} - f\frac{\Gamma_*}{C_a} - [1 - \frac{\delta^{13}C_{air}+1}{\delta^{13}C_{sub}+1}(1+e)]\frac{R_d}{kC_a}\}, \quad (6)$$

where Γ_* (μmol mol^{-1}) is the CO_2 compensation point in the absence of dark respiration (Bernacchi et al. 2001); $k=(A_n + R_d)/(C_c - \Gamma_*)$ (mol m^{-2} s^{-1}) is the carboxylation efficiency. More details on model parameterization and evaluation were presented in studies I and II.

The two studies differed in the following aspects: (1) the boundary layer effects were omitted in study I but not in study II; (2) a constant g_m value (Stangl et al. 2019) was used in study I, while dynamic g_m values (Dewar et al. 2018) were used in study II; (3) in study II the respiratory substrate was assumed to be the leaf sugar pool instead of the new assimilates as in study I; (4) input gas exchange data were obtained from online shoot gas exchange measurements in study I, but modelled based on environmental data in study II; (5) modelled

$\delta^{13}C_A$ was compared directly with leaf sucrose $\delta^{13}C$ in study I, whereas in study II $\delta^{13}C$ of leaf sugars was predicted dynamically with leaf sugar pool size considered.

In study I, model uncertainty might rise from the ignorance of boundary layer effects, the simplification of g_m dynamics and the assumption that respiration substrates were new assimilates, which is in contrast to the finding of Busch et al. (2020). Additionally, ternary effects likely affected the results of study I, but should have less impact on study II, where it was consistently ignored in simulating both gas exchange and ^{13}C discrimination (Farquhar and Cernusak 2012).

3.7 iWUE estimation

Half-hourly input data were used for iWUE estimation, and the results were averaged to daytime means (studies I and IV).

3.7.1 iWUE from gas exchange data

iWUE was calculated from shoot gas exchange data ($iWUE_{gas}$) according to Eq. 7, for years from 2002 to 2019 in both sites, but not for 2005 or 2014 in Hyytiälä due to data gaps.

$$iWUE_{gas}=A_n/E\cdot(VPD/P_a), \quad (7)$$

where P_a is atmospheric pressure.

3.7.2 iWUE from $\delta^{13}C$ data

iWUE was estimated from $\delta^{13}C$ data ($iWUE_{iso}$) according to Eq. 8.

$$iWUE_{iso}=(C_a - C_i)/1.6 \quad (8)$$

For a simple $iWUE_{iso}$ estimation model, C_i was estimated from Eqs. 2 and 3. For a complex model with the incorporation of g_m and photorespiration, C_i was estimated from Eqs. 2 and 5, assuming R_d=0 in study IV. Availability and processing of input data were described in studies I and IV.

3.7.3 iWUE from eddy covariance data

iWUE was calculated from eddy covariance data ($iWUE_{EC}$) according to Eq. 9.

$$iWUE_{EC}=GPP/ET\cdot(VPD/P_a) \quad (9)$$

Gross primary production (GPP) was calculated by subtracting the modelled total ecosystem respiration from measured net ecosystem CO_2 exchange (Kulmala et al. 2019). Net ecosystem CO_2 exchange and ecosystem H_2O flux (ET) were measured via a closed-path eddy covariance system above the stand at 24 m height from 2002 to 2017 in Hyytiälä, at 27 m height from 2018 to 2019 in Hyytiälä, and at 16.6 m from 2012 to 2019 in Värriö. More detailed description of the eddy covariance system can be found in Vesala et al. (2005), and eddy covariance data processing in study IV.

4. RESULTS AND DISCUSSION

4.1 Improved understanding of photosynthetic isotope discrimination

4.1.1 Impacts of mesophyll conductance

Although it has been acknowledged that g_m may constrain photosynthetic rate and thereby $\delta^{13}C_A$ by Evans et al. already in 1986, g_m was for a long time not explicitly incorporated in isotope discrimination models. Studies I and II demonstrate that explicitly accounting for g_m dynamics is crucial for interpreting leaf-level $\delta^{13}C$ signals at intra-seasonal scale. Study I applied a constant g_m value in the isotope discrimination model, which resulted in an overall agreement between modelled $\delta^{13}C_A$, chamber-based $\delta^{13}C_A$ and leaf sucrose $\delta^{13}C$ in both absolute values and seasonal variability for most of the growing season, but not for the hottest period (Figure 6). This discrepancy at high temperatures can be at least partly attributed to a dynamic intra-seasonal pattern of g_m, which tends to increase sharply with temperature (von Caemmerer and Evans 2015; Shrestha et al. 2019). Indeed, the assumption of a dynamic g_m in proportion to $A_n/(C_c - \Gamma_*)$ (Dewar et al. 2018) produced better model agreements than the assumption of a constant g_m value (Wingate et al. 2007; Ogée et al. 2009) in study II. Although accounting for the seasonal variability of g_m is ideal for modelling $\delta^{13}C_A$ and iWUE, as suggested by study II and Gimeno et al. (2021), incorporating a constant g_m value is undoubtedly better than incorporating none.

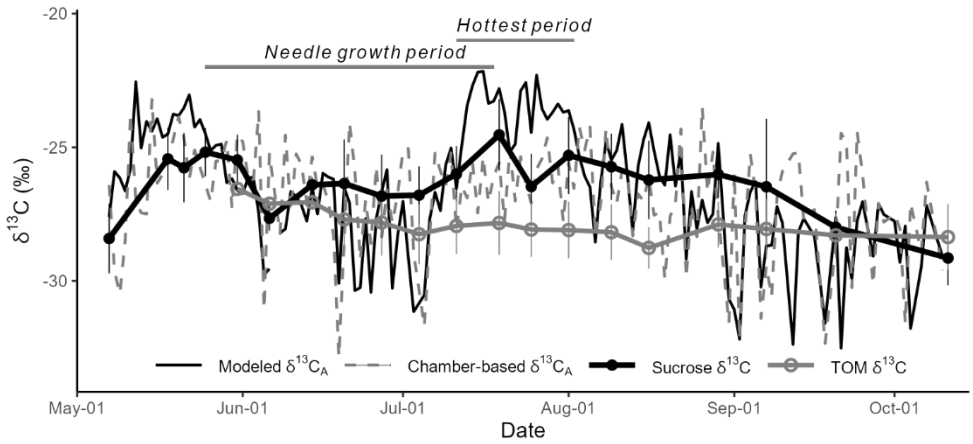

Figure 6. Comparison of modelled and chamber-based $\delta^{13}C$ of new assimilates ($\delta^{13}C_A$) and $\delta^{13}C$ of leaf sucrose and total organic matter (TOM) of Scots pine in Hyytiälä during the growing season of 2018. Error bars represent SD of five trees. Revised from Figure 3 of study I.

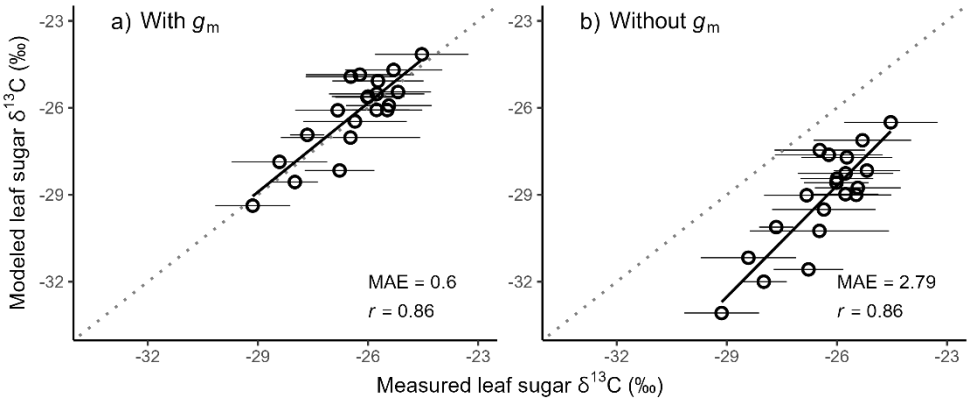

Figure 7. The fit between modelled and measured $\delta^{13}C$ of leaf sugar when g_m was (a) and was not (b) incorporated in the isotope discrimination model. The dashed line is 1:1 and the solid line the linear least squares regression. Mean absolute error (MAE) and *r* of the model fit are given. Error bars represent SD of five trees. Revised from Figure 4 of study II.

When g_m was neglected in the isotope discrimination model, $\delta^{13}C$ of leaf sugars was clearly underestimated and the mean absolute error of the model fit increased (Figure 7). In consequence, nonexplicit consideration of g_m contributed to an overestimation of $\delta^{13}C$-based iWUE by 9% at leaf level (study I) and 7% at tree-ring level (study IV). Nevertheless, it is worth noting that the impact of g_m on iWUE estimates was much less significant than detected for other species, such as up to 65% reported for crop species by Ma et al. (2021), probably due to a species-specific pattern in g_m dynamics (Ubierna et al. 2017). Hence, estimating iWUE in a simplified manner via Eqs. 2, 3 and 8 may be a plausible compromise for boreal Scots pine, albeit not for species that have demonstrated a significant impact of g_m on iWUE estimates, if no instrumental data are available for the incorporation of g_m into the iWUE model.

4.1.2 Impacts of carry-over effect of leaf sugars

The carry-over effect of leaf assimilates was considered with two different assumptions: a constant proportion of current-day formed sugars was preserved in the leaf to the following day (study I) or the leaf sugar pool was of a constant size with well-mixed new and old assimilates (study II). Based on these assumptions, weighted means of past environmental and physiological parameters were calculated and their correlations with leaf sugar $\delta^{13}C$ were computed. When the carry-over effect of leaf assimilates was considered, stronger correlations were obtained between $\delta^{13}C$ of leaf sugars and environmental variables (Figure 8) or C_i/C_a (Figure 9). Likewise, Brendel et al. (2003) found $\delta^{13}C$ of leaf TOM correlated better with integrated environmental variables over past days than daily index. Study I showed a carry-over effect of from 3 to 5 d for leaf sucrose, while study II suggested that the leaf sugar pool was a composite of sugars formed between 2 to over 5 d. These results are in line with the finding of Desalme et al. (2017) that the mean residence time of the ^{13}C labels in WSCs in one-year-old needles varied between 1 d to 5 d, depending on the time of the growing season, after $^{13}CO_2$ pulse-labelling of *Pinus pinaster*. Furthermore, this carry-over effect also corresponds to the suggestion of a two-compartment pool of sucrose in leaf cells:

a slow transport pool in vacuole and a fast transport pool in cytosol (Kouchi and Yoneyama 1984; Brauner et al. 2014). Our finding that from 70% to 80% of current-day formed sucrose is preserved in leaves (Figure 8) agrees well with a previous suggestion that from 40% to 80% of sucrose is stored in vacuole of various non-tree plant species (Nadwodnik and Lohaus 2008).

Due to the carry-over effect of leaf sugars, the seasonal and diurnal variations of leaf sugar $\delta^{13}C$ were not as strong as that of chamber-based $\delta^{13}C_A$ (studies I and II). Moreover, $\delta^{13}C$ of leaf sugars was ca. 1‰ lower than chamber-based $\delta^{13}C_A$ in the early afternoon, due to the accumulation of relatively ^{13}C-depleted sugars assimilated in the morning. These pieces of evidence underline that explicit consideration of the temporal mixing of sugars in leaves is important for reliable interpretation of the dynamics in leaf $\delta^{13}C$ signal. Moreover, studies I and II show the potential of combining an isotope discrimination model, online chamber-based $\delta^{13}C$ analysis of CO_2 flux and CSIA of leaf sugars in examining temporal dynamics of sugar export from leaves to phloem (opposite to the carry-over effect in leaves). Such information on sugar export has been examined via $^{13}CO_2$ pulse-labelling experiments (Epron et al. 2012), however, often confined to small trees.

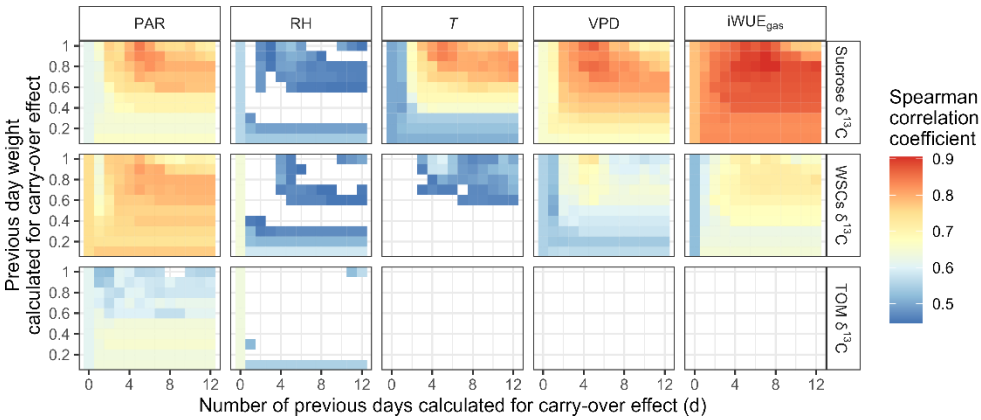

Figure 8. Environmental and physiological signals imprinted in $\delta^{13}C$ of leaf sucrose, water-soluble carbohydrates (WSCs), and total organic matter (TOM) of Scots pine in Hyytiälä during the growing season of 2018. The carry-over effect was calculated by integrating the environmental and physiological variables over previous days with varying weights (study I). The *x*-axis represents the number of days calculated for the carry-over effect, and the *y*-axis represents the percentage of current-day leaf carbon pools that were reserved in the following day. PAR is photosynthetically active radiation, *T* is temperature, RH is relative humidity, VPD is vapor pressure deficit, and $iWUE_{gas}$ is intrinsic water use efficiency estimated from leaf gas exchange data. Only significant results ($P<0.05$) are presented. Spearman's correlation coefficient is indicated by the colors from blue (low values) to red (high values). Revised from Figure 4 of study I.

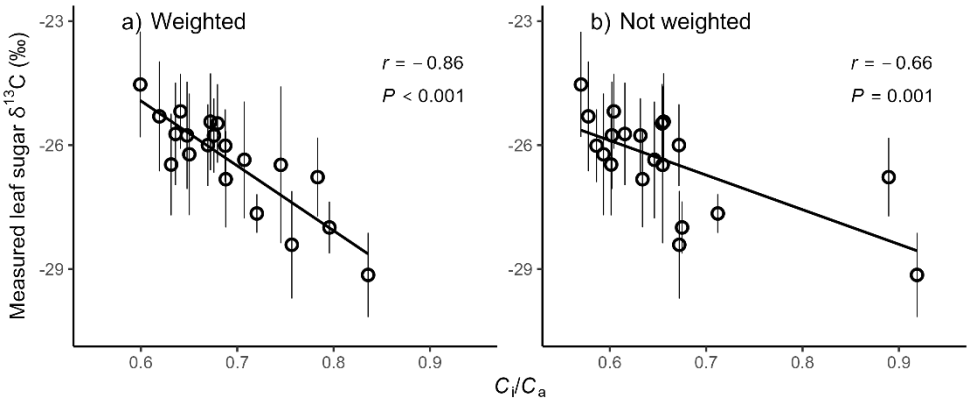

Figure 9. Relationship between modelled intercellular to ambient CO_2 concentration ratio (C_i/C_a) and measured leaf sugar $\delta^{13}C$, when time integration was (a) or was not (b) considered in C_i/C_a. The solid line is the linear least squares regression. Correlation coefficient *r* and *P*-value are presented. Error bars represent SD of five trees. Revised from Figure 8 of study II.

4.2 Improved understanding of post-photosynthetic processes

4.2.1 $\delta^{13}C$ offsets between carbon pools and respired CO_2

Unlike sucrose, all other examined leaf carbon pools, that is, pinitol, starch, WSCs and TOM, showed significant and seasonally varying $\delta^{13}C$ offsets from modelled and chamber-based $\delta^{13}C_A$ (study I). On the one hand, the result implies that $\delta^{13}C$ of leaf sucrose provides a rather accurate estimate for $\delta^{13}C_A$. On the other hand, the result reflects isotopic fractionation during enzyme-catalyzed synthesis of other metabolites. Compared with modelled and chamber-based $\delta^{13}C_A$, $\delta^{13}C$ of pinitol, WSCs and TOM were over 3, 1.5 and 1‰ lower, respectively, whereas $\delta^{13}C$ of starch was ca. 1‰ higher. These offsets are in line with previous investigations (Figure 2).

Leaf assimilates are subsequently exported to phloem, mainly in the form of sucrose (Rennie and Turgeon 2009; Julius et al. 2017). However, $\delta^{13}C$ of phloem sucrose at breast height was ca. 1‰ higher relative to leaf sucrose assimilated at top canopy (Figure 10). This offset likely results from the refixation of ^{13}C-enriched CO_2 associated with PEPc activity (Gessler et al. 2009a) and the contribution of ^{13}C-enriched transitory starch to exported sucrose (Gessler and Ferrio 2022). This offset is also partly counterbalanced by the integration of sucrose produced at lower canopy with lower $\delta^{13}C$ signal due to lower light availability (Le Roux et al. 2001). Furthermore, from phloem sucrose to resin-extracted tree-ring (consisting of cellulose and lignin), $\delta^{13}C$ decreased by ca. 0.5‰ (Figure 10), possibly due to fractionation against ^{13}C during lignin formation (Hobbie and Werner 2004). Taken together, the overall ^{13}C-enrichment relative to leaf sucrose was ca. 0.5‰ for resin-extracted tree-ring, and ca. 2‰ for wood cellulose if the $\delta^{13}C$ difference between cellulose and resin-extracted tree-ring was considered (Schulze et al. 2004). Accounting for these $\delta^{13}C$ offsets is crucial for accurate interpretation of tree-ring $\delta^{13}C$-derived iWUE values (study IV).

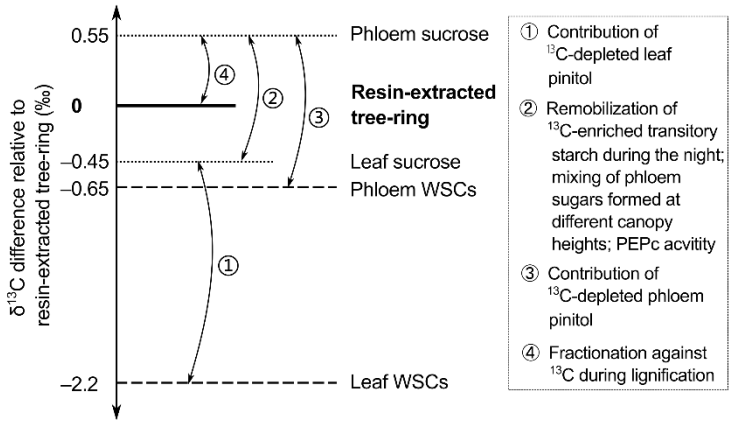

Figure 10. $\delta^{13}C$ difference between resin-extracted tree-ring and tree sugar pools together with possible underlying mechanisms. WSCs is water-soluble carbohydrates; PEPc is phospho*enol*pyruvate carboxylase. Average values from seasonal sampling in Hyytiälä and Värriö are presented, modified from Figure 5 of Study IV.

Previous studies reported contradictory results on the direction of $\delta^{13}C$ difference between stem or root respired CO_2 and respiratory substrates (Section 1.2.3). This discrepancy very likely results from the fact that different carbon pools, most often bulk matter such as WSOM or TOM, were analyzed in different studies as respiratory substrates. Bulk matter consists of a mixture of organic compounds, which have distinct $\delta^{13}C$ values (Figure 2). In fact, a significant proportion of the bulk matter, such as structural compounds or mobile compounds with long turnover rates, is not likely to be the substrate for respiration under normal conditions. In comparison, sucrose can provide a more accurate estimate for the $\delta^{13}C$ value of the respiratory substrate. CSIA data in study III depicted a clear ^{13}C-depletion of stem respired CO_2 relative to phloem WSCs and sucrose. This fractionation is possibly linked to the release of CO_2 from ^{13}C-depleted C-1 position of glucose via oxidative pentose phosphate pathway (Rossmann et al. 1991; Bathellier et al. 2008) and preferential refixation of $^{13}CO_2$ via PEPc activity (Farquhar 1983; Gessler et al. 2009a). ^{13}C-depletion of soil respired CO_2 relative to root WSCs was also detected in study III, but an in-depth understanding of the fractionation process would rely on a careful separation of autotrophic respiration from heterotrophic respiration and a thorough $\delta^{13}C$ determination of soil carbon pools.

Summarizing, studies I, III and IV point out that the $\delta^{13}C$ signal in bulk matter, such as WSCs and TOM, may be strongly biased due to the mixing of different compounds, and that careful interpretation is needed, if environmental and physiological information is derived from bulk $\delta^{13}C$ signal. CSIA thereby confers an improved ability to decipher photosynthetic and post-photosynthetic isotope discrimination processes than conventional bulk isotope analysis.

4.2.2 No significant use of reserves

In the present thesis, no clear sign of use of reserves was detected for needle growth (study I), tree-ring growth (study IV) and root growth (study III) of mature Scots pine trees. These findings indicate that there may be a better chance to use Scots pine for paleoenvironmental

research than other species, for instance, deciduous trees (Villar-Salvador et al. 2015; Vincent-Barbaroux et al. 2019), which have shown significant use of reserves.

At leaf level, $\delta^{13}C$ of TOM in developing needles aligned with modelled and chamber-based $\delta^{13}C_A$ in both absolute values and temporal variations during the initial stage of leaf flush (Figure 6), suggesting use of new assimilates rather than old reserves for needle growth. Low dependence of leaf growth on reserves has been reported also for mature evergreen conifer *Pinus uncinata* Ramond (von Felten et al. 2007), mature deciduous conifer *Larix gmelinii* (Rinne et al. 2015b), as well as for a variety of deciduous and evergreen broadleaf species (Villar-Salvador et al. 2015). For these deciduous trees, expanding leaves become autotrophic rapidly after budburst, and thus the degree of use of reserves for total leaf biomass growth is low (Rinne et al. 2015b; Villar-Salvador et al. 2015). By contrast, significant reliance on stored carbon for leaf development was reported for mature deciduous *Larix decidua* (von Felten et al. 2007), *Larix gmelinii* saplings (Kagawa et al. 2006), mature deciduous oaks *Quercus alba* and *Quercus prinus* (Gaudinski et al. 2009), deciduous savanna tree species *Terminalia sericea* and *Combretum apiculatum* (February and Higgins 2016), and mature evergreen *Pinus pinaster* (Desalme et al. 2017). It seems increasingly obvious that the use of reserves for leaf growth is not solely dependent on plant functional types or tree ages, but also on the environment the trees live in and the strategy they take for better survival.

Regarding tree-ring growth, no clear use of reserves was detected for Scots pine in either study site (study IV). In previous studies, the reliance of reserve carbohydrates for earlywood growth was often supported by a significant correlation between $\delta^{13}C$ across the ring border, such as for *Picea abies* (Vaganov et al. 2009) and *Pinus sylvestris* (Fonti et al. 2018), or by a high $\delta^{13}C$ signal in earlywood originating from potential use of ^{13}C-enriched starch reserves (Jäggi et al. 2002). In study IV, however, there were no significant correlations between $\delta^{13}C$ across the ring border, after applying first-differencing to remove the low-frequency trends in $\delta^{13}C$ chronologies, as suggested by McCarroll et al. (2017). Additionally, an overall agreement of intra-seasonal variability between leaf-level $iWUE_{gas}$ and tree-level $iWUE_{iso}$ at both sites suggests a synchrony of $\delta^{13}C$ dynamics between new assimilates and tree-rings. Aside from the fact that the low-frequency trends were not removed in previous studies (Vaganov et al. 2009; Fonti et al. 2018), the contradiction between previous findings and our results may also indicate a species-specific and environment-dependent carbon use strategy for wood formation. As observed by Bryukhanova et al. (2011) and Vincent-Barbaroux et al. (2019), species differ significantly in the use of reserves for earlywood growth, depending on the balance between photosynthetic supply and growth demands.

Two lines of evidence in Study III suggest that root growth of Scots pine in Hyytiälä was mainly dependent on new assimilates. First, there was a significant correlation between the rate of root growth and the concentration of root starch, as also observed by Wang et al. (2018). Second, root starch mainly originated from new assimilates rather than stored carbon, as starch content was very low before the first root flush and showed a similar temporal pattern with WSC content. Our finding is consistent with the previous report that fresh assimilates are intricately involved in new root growth of conifers, whereas the initial root growth of deciduous trees relies on old reserves as their root elongation resumes before budburst (Villar-Salvador et al. 2015).

4.3 Tree $\delta^{13}C$ for environmental and physiological studies

4.3.1 Weaker environmental signal in $\delta^{13}C$ of bulk matter

A weaker or even distorted environmental signal was detected in $\delta^{13}C$ of leaf pinitol, starch, WSCs and TOM (Figure 8, study I), in comparison with $\delta^{13}C$ of sucrose. The distorted environmental signal in $\delta^{13}C$ of pinitol is caused by the slow turnover rate of this compound (Streeter et al. 2001), which is decoupled from the flow of new assimilates (Kouchi and Yoneyama 1984). Consequently, due to the commonly high proportion (ca. 40% in our data) of pinitol in a WSC pool, environmental signal is also dampened in $\delta^{13}C$ of WSCs. Not surprisingly, it can be expected that environmental signal is further distorted in $\delta^{13}C$ of WSOM and TOM, because of the presence of several other compounds, which have different $\delta^{13}C$ values from $\delta^{13}C_A$ (Bowling et al. 2008; Figure 2). Also, the accumulation of starch over time results in mixing of carbon formed at different times in the starch pool, hence the lack of environmental signal in starch $\delta^{13}C$.

Similarly, physiological information, such as iWUE, was also dampened in $\delta^{13}C$ of leaf bulk matter (Figure 8, study I). Likewise, Merchant et al. (2011) found that changes in $\delta^{13}C$ of leaf WSOM were much less coupled to changes in C_i/C_a compared with $\delta^{13}C$ of leaf or phloem sucrose. Resultantly, $\delta^{13}C$ of leaf bulk matter may fail to capture the seasonal dynamics of iWUE (Figure 11; Tarin et al. 2020), or produce biased iWUE values (Figure 11; Stoke et al. 2010), due to the $\delta^{13}C$ offset between leaf bulk matter and new assimilates.

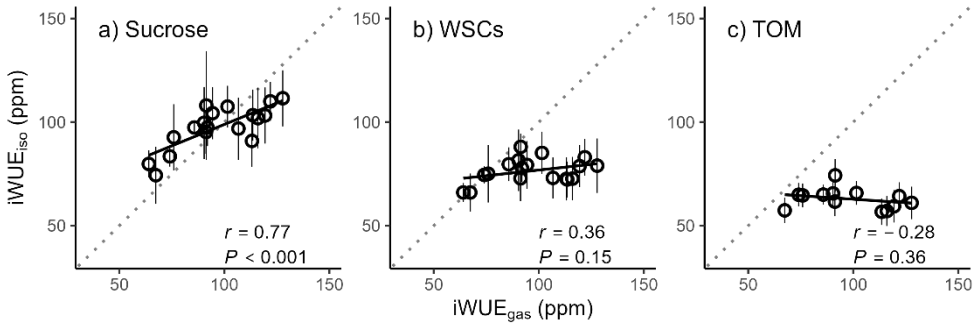

Figure 11. Relationship between intrinsic water use efficiency derived from leaf gas exchange ($iWUE_{gas}$) and $\delta^{13}C$ ($iWUE_{iso}$) of (a) sucrose, (b) water-soluble carbohydrates (WSCs) and (c) total organic matter (TOM) in leaves. The dotted line is 1:1 and the solid line the linear least squares regression. Correlation coefficient *r* and *P*-value are presented. Error bars represent SD of five trees. Revised from Figure 5 of Study I.

4.3.2 iWUE estimates from tree-ring $\delta^{13}C$

Considering that $\delta^{13}C$ of leaf sucrose provides a rather accurate estimate of leaf-level iWUE at intra-seasonal scale (Figure 11; study I) and that sucrose $\delta^{13}C$ is transported to and laid down in tree-rings (Gessler et al. 2009b; Rinne et al. 2015a), there should be a high potential to estimate intra-seasonal iWUE signal from tree-ring $\delta^{13}C$ data. In study IV, with the aid of LA-IRMS analysis of tree-rings, high-resolution intra-seasonal $iWUE_{iso}$ was estimated for Värriö and Hyytiälä from 2002 to 2019. For both sites, the intra-seasonal pattern of $iWUE_{iso}$ agreed generally well with that of $iWUE_{gas}$ and $iWUE_{EC}$ (Figure 12), when yearly tree-ring growth was carefully determined to time $iWUE_{iso}$. This agreement supports the reliability of tree-ring $\delta^{13}C$ data for detecting iWUE dynamics at high-resolution intra-seasonal scale. The main advantage of tree-ring $\delta^{13}C$ data is that the signal is archived in tree-rings which exist for a wide range of areas and periods and can be retrieved even decades and centuries after tree-ring formation without laborious work on site (Cernusak 2020). Therefore, this finding is of high significance, especially to studies which seek to detect short-term dynamics of water and carbon trade but have no access to gas exchange or eddy covariance data.

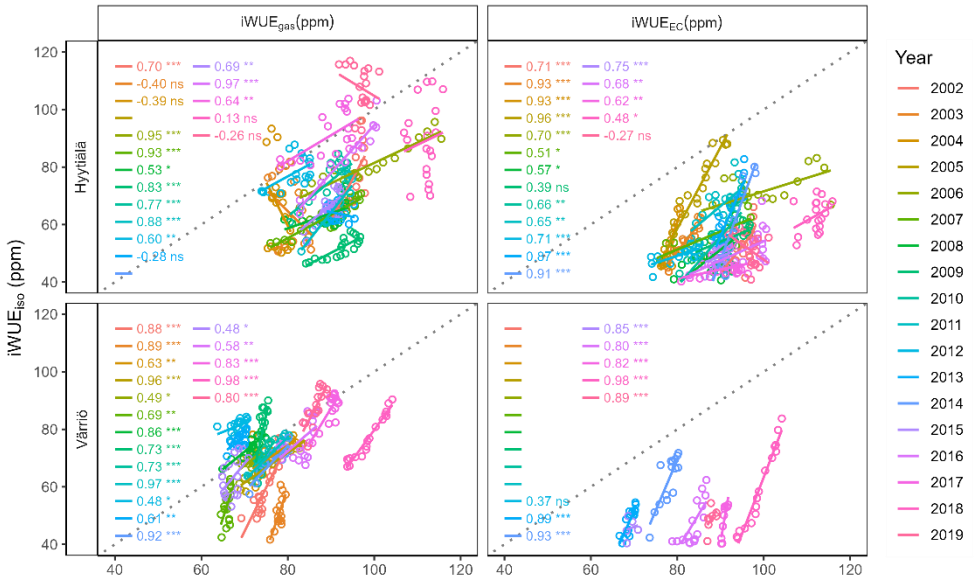

Figure 12. Relationships between intra-seasonal intrinsic water use efficiency derived from tree-ring $\delta^{13}C$ ($iWUE_{iso}$), leaf gas exchange ($iWUE_{gas}$) and eddy covariance ($iWUE_{EC}$) data for Hyytiälä and Värriö during years from 2002 to 2019. The dotted line is 1:1, and the solid line are linear least squares regressions for each year and site. Correlation coefficient *r* and significance level (*** $P<0.001$, ** $0.001 \leq P<0.01$, * $0.01 \leq P<0.05$, and ns $P \geq 0.05$) are presented.

However, there were differences between $iWUE_{iso}$, $iWUE_{gas}$ and $iWUE_{EC}$ in absolute values, inter-annual trends and in some cases intra-seasonal patterns (study IV), which can be ascribed to the following reasons. First, these discrepancies can rise from uncertainties of each iWUE estimation method. For example, $iWUE_{iso}$ was overestimated by up to 11% due to post-photosynthetic $\delta^{13}C$ alteration, and by up to 14% due to nonexplicit consideration of mesophyll and photorespiratory effects. $iWUE_{EC}$ estimates are likely biased due to energy imbalance, neglection of daytime canopy respiration in GPP estimation, canopy gradients and contribution of non-transpiratory water fluxes (Medlyn et al. 2017; Knauer et al. 2018). $iWUE_{gas}$ estimates are impacted by chamber artifacts, which cause differences in conditions inside and outside the chamber, limited sampling coverage, and low consistency in measurement systems in long term. Second, environmental variables may have varying impacts on the three iWUE estimates, which represent signals at different scales. For instance, the tree-level $iWUE_{iso}$ is less impacted by C_a than the top canopy leaf-level $iWUE_{gas}$, because photosynthesis within the canopy is predominantly limited by ribulose 1,5-bisphosphate regeneration, which is less sensitive to C_a compared with Rubisco-limited photosynthesis at the top canopy (Yang et al. 2020). Additionally, the ecosystem-level $iWUE_{EC}$ integrates the species-specific physiological response to environmental stresses across various plant species over the stand (Yi et al. 2019), and thus may vary in a different manner than $iWUE_{gas}$ and $iWUE_{iso}$ that represent the signal of the studied species only.

Study IV not only extends the application of tree-ring $\delta^{13}C$ data for iWUE reconstructions from the conventional annual resolution (Frank et al. 2015; Adams et al. 2020; Mathias and Thomas 2021) to high-resolution intra-seasonal scale, but also presents the first example for across-method comparisons of iWUE at various temporal scales. Such comparison for longer time series and at more study sites can provide further insights in the scale-specific physiological acclimation of trees under climate change and in the upscaling of ecological models.

5. CONCLUSIONS

This thesis combined CSIA of sugars with online chamber-based $\delta^{13}C$ analysis of CO_2 flux and isotope discrimination models, in the effort to better understand the photosynthetic and post-photosynthetic isotope fractionation processes. The obtained knowledge was further applied to extract physiological information from LA-IRMS-derived tree-ring $\delta^{13}C$ data. The main findings of this thesis include the following aspects.

First, g_m dynamics had a significant impact on the output of isotope discrimination models. g_m was not constant over the growing season but seemed to vary considerably in response to environmental changes, such as temperature, although incorporating a constant g_m value in models was no doubt better than neglecting g_m. If g_m was not accounted for, iWUE derived from leaf $\delta^{13}C$ tended to be overestimated, but the degree of overestimation was less significant for Scots pine than reported for other species. Second, assimilates tended to preserve in the leaves for 2 to 5 d. This short-term carry-over effect dampened the strength of current-day environmental signal imprinted in $\delta^{13}C$ of leaf sugars. Accounting for this carry-over effect in the isotope discrimination model is important for predicting the intra-seasonal dynamics of leaf sugar $\delta^{13}C$. Third, no significant use of reserves was detected for the biomass growth of needles or roots of Scots pine in Hyytiälä during the growing season of 2018, or for stem growth of Scots pine at Hyytiälä and Värriö over the years from 2002 to 2019. Therefore, boreal Scots pine may be a better choice for tree-ring $\delta^{13}C$-based reconstructions of environmental and physiological variables, in comparison with species that have shown considerable degree of use of reserves. Fourth, $\delta^{13}C$ of leaf bulk matter significantly deviated from the modelled and chamber-based $\delta^{13}C_A$, resulting in reduced or even distorted environmental and physiological signals in $\delta^{13}C$ of leaf bulk matter. In comparison, leaf sucrose $\delta^{13}C$ documented leaf-level iWUE, as well as other environmental variables, in a highly accurate manner. $\delta^{13}C$ of leaf sucrose is transported to tree-rings, hence laying the basis for tree-ring $\delta^{13}C$-based iWUE reconstructions. Fifth, the intra-seasonal patterns of iWUE derived from tree-ring $\delta^{13}C$ aligned well with that estimated from gas exchange and eddy covariance data during years from 2002 to 2019 for both study sites. However, the inter-annual trends of iWUE were different between the estimation methods, mainly due to diverse environmental drivers on changes of each iWUE estimate.

Taking advantage of CSIA and LA-IRMS, this thesis not only deepens our understanding of the less well-known aspects in photosynthetic and post-photosynthetic isotope discrimination processes, but also extends the application of tree-ring $\delta^{13}C$-based iWUE estimation to intra-seasonal scale. Future studies can further benefit from the two methodological tools, for example, in separating the impact of individual metabolic processes on post-photosynthetic $\delta^{13}C$ alteration from leaf assimilates to tree-rings, by combining intra-seasonal CSIA data in leaves and phloem, intra-ring LA-IRMS data and enzyme activity measurements.

REFERENCES

Aaltonen H, Aalto J, Kolari P, Pihlatie M, Pumpanen J, Kulmala M, Nikinmaa E, Vesala T, Bäck J (2013) Continuous VOC flux measurements on boreal forest floor. Plant Soil 369: 241–256. https://doi.org/10.1007/s11104-012-1553-4.

Adams MA, Buckley TN, Turnbull TL (2020) Diminishing CO_2-driven gains in water-use efficiency of global forests. Nat Clim Chang 10: 466–471. https://doi.org/10.1038/s41558-020-0747-7.

Altimir N, Kolari P, Tuovinen J, Vesala T, Bäck J, Suni T, Kulmala M, Hari P (2006) Foliage surface ozone deposition: a role for surface moisture? Biogeosciences 3: 209–228. https://doi.org/10.5194/bg-3-209-2006.

Altimir N, Vesala T, Keronen P, Kulmala M, Hari P (2002) Methodology for direct field measurements of ozone flux to foliage with shoot chambers. Atmos Environ 36: 19–29. https://doi.org/10.1016/S1352-2310(01)00478-2.

Aubrey DP, Teskey RO (2018) Stored root carbohydrates can maintain root respiration for extended periods. New Phytol 218: 142–152. https://doi.org/10.1111/nph.14972.

Badeck FW, Tcherkez G, Nogués S, Piel C, Ghashghaie J (2005) Post-photosynthetic fractionation of stable carbon isotopes between plant organs – a widespread phenomenon. Rapid Commun Mass Spectrom 19: 1381–1391. https://doi.org/10.1002/rcm.1912.

Barbour MM, Mcdowell NG, Tcherkez G, Bickford CP, Hanson DT (2007) A new measurement technique reveals rapid post-illumination changes in the carbon isotope composition of leaf-respired CO_2. Plant Cell Environ 30: 469–482. https://doi.org/10.1111/j.1365-3040.2007.01634.x.

Barrie A, Bricout J, Koziet J (1984) Gas chromatography – stable isotope ratio analysis at natural abundance levels. Biol Mass Spectrom 11: 583–588. https://doi.org/10.1002/bms.1200111106.

Bathellier C, Badeck F, Couzi P, Harscoët S, Mauve C, Ghashghaie J (2008) Divergence in $\delta^{13}C$ of dark respired CO_2 and bulk organic matter occurs during the transition between heterotrophy and autotrophy in *Phaseolus vulgaris* plants. New Phytol 177: 406–418. https://doi.org/10.1111/j.1469-8137.2007.02246.x.

Battipaglia G, De Micco V, Brand WA, Linke P, Aronne G, Saurer M, Cherubini P (2010) Variations of vessel diameter and $\delta^{13}C$ in false rings of *Arbutus unedo* L. reflect different environmental conditions. New Phytol 188: 1099–1112. https://doi.org/10.1111/j.1469-8137.2010.03443.x.

Bernacchi CJ, Singsaas EL, Pimentel C, Portis Jr AR, Long SP (2001) Improved temperature response functions for models of Rubisco-limited photosynthesis. Plant Cell Environ 24: 253–259. https://doi.org/10.1111/j.1365-3040.2001.00668.x.

Bögelein R, Lehmann MM, Thomas FM (2019) Differences in carbon isotope leaf-to-phloem fractionation and mixing patterns along a vertical gradient in mature European beech and Douglas fir. New Phytol 222: 1803–1815. https://doi.org/10.1111/nph.15735.

Boschker HTS, Moerdijk-Poortvliet TCW, van Breugel P, Houtekamer M, Middelburg JJ (2008) A versatile method for stable carbon isotope analysis of carbohydrates by high-performance liquid chromatography/isotope ratio mass spectrometry. Rapid Commun Mass Spectrom 22: 3902–3908. https://doi.org/10.1002/rcm.3804.

Bowling DR, Pataki DE, Randerson JT (2008) Carbon isotopes in terrestrial ecosystem pools and CO_2 fluxes. New Phytol 178: 24–40. https://doi.org/10.1111/j.1469-8137.2007.02342.x.

Brandes E, Kodama N, Whittaker K, Weston C, Rennenberg H, Keitel C, Adams MA, Gessler A (2006) Short-term variation in the isotopic composition of organic matter allocated from the leaves to the stem of *Pinus sylvestris*: effects of photosynthetic and postphotosynthetic carbon isotope fractionation. Glob Change Biol 12: 1922–1939. https://doi.org/10.1111/j.1365-2486.2006.01205.x.

Brauner K, Hörmiller I, Nägele T, Heyer AG (2014) Exaggerated root respiration accounts for growth retardation in a starchless mutant of *Arabidopsis thaliana*. Plant J 79: 82–91. https://doi.org/10.1111/tpj.12555.

Brendel O, Handley L, Griffiths H (2003) The $\delta^{13}C$ of Scots pine (*Pinus sylvestris* L.) needles: spatial and temporal variations. Ann For Sci 60: 97–104. https://doi.org/10.1051/forest:2003001.

Bryukhanova MV, Vaganov EA, Wirth C (2011) Influence of climatic factors and reserve assimilates on the radial growth and carbon isotope composition in tree rings of deciduous and coniferous species. Contemp Probl Ecol 4: 126–132. https://doi.org/10.1134/S1995425511020020.

Busch FA, Holloway-Phillips M, Stuart-Williams H, Farquhar GD (2020) Revisiting carbon isotope discrimination in C3 plants shows respiration rules when photosynthesis is low. Nat Plants 6: 245–258. https://doi.org/10.1038/s41477-020-0606-6.

Cernusak LA (2020) Gas exchange and water-use efficiency in plant canopies. Plant Biol J 22: 52–67. https://doi.org/10.1111/plb.12939.

Cernusak LA, Ubierna N, Winter K, Holtum JAM, Marshall JD, Farquhar GD (2013) Environmental and physiological determinants of carbon isotope discrimination in terrestrial plants. New Phytol 200: 950–965. https://doi.org/10.1111/nph.12423.

Churakova (Sidorova) O, Lehmann M, Saurer M, Fonti M, Siegwolf R, Bigler C (2018) Compound-specific carbon isotopes and concentrations of carbohydrates and organic acids as indicators of tree decline in mountain pine. Forests 9, article id 363. https://doi:10.3390/f9060363.

Churakova (Sidorova) OV, Lehmann MM, Siegwolf RTW, Saurer M, Fonti MV, Schmid L, Timofeeva G, Rinne-Garmston KT, Bigler C (2019) Compound-specific carbon isotope patterns in needles of conifer tree species from the Swiss National Park under recent climate change. Plant Physiol Biochem 139: 264–272. https://doi.org/10.1016/j.plaphy.2019.03.016.

Damesin C, Lelarge C (2003) Carbon isotope composition of current-year shoots from *Fagus sylvatica* in relation to growth, respiration and use of reserves. Plant Cell Environ 26: 207–219. https://doi.org/10.1046/j.1365-3040.2003.00951.x.

Danielewska A, Urbaniak M, Olejnik J (2015) Growing season length as a key factor of cumulative net ecosystem exchange over the pine forest ecosystems in Europe. Int Agrophysics 29: 129–135. https://doi.org/10.1515/intag-2015-0026.

De Micco V, Battipaglia G, Brand WA, Linke P, Saurer M, Aronne G, Cherubini P (2012) Discrete versus continuous analysis of anatomical and $\delta^{13}C$ variability in tree rings with intra-annual density fluctuations. Trees 26: 513–524. https://doi.org/10.1007/s00468-011-0612-4.

Desalme D, Priault P, Gérant D, Dannoura M, Maillard P, Plain C, Epron D (2017) Seasonal variations drive short-term dynamics and partitioning of recently assimilated carbon in the foliage of adult beech and pine. New Phytol 213: 140–153. https://doi.org/10.1111/nph.14124.

Dewar R, Mauranen A, Mäkelä A, Hölttä T, Medlyn B, Vesala T (2018) New insights into the covariation of stomatal, mesophyll and hydraulic conductances from optimization models incorporating nonstomatal limitations to photosynthesis. New Phytol 217: 571–585. https://doi.org/10.1111/nph.14848.

Duranceau M, Ghashghaie J, Badeck F, Deleens E, Cornic G (1999) $\delta^{13}C$ of CO_2 respired in the dark in relation to δ^{13} C of leaf carbohydrates in *Phaseolus vulgaris* L. under progressive drought. Plant Cell Environ 22: 515–523. https://doi.org/10.1046/j.1365-3040.1999.00420.x.

Epron D, Bahn M, Derrien D, Lattanzi FA, Pumpanen J, Gessler A, Hogberg P, Maillard P, Dannoura M, Gerant D, Buchmann N (2012) Pulse-labelling trees to study carbon allocation dynamics: a review of methods, current knowledge and future prospects. Tree Physiol 32: 776–798. https://doi.org/10.1093/treephys/tps057.

Evans JR, Sharkey TD, Berry JA, Farquhar GD (1986) Carbon isotope discrimination measured concurrently with gas exchange to investigate CO_2 diffusion in leaves of higher plants. Funct Plant Biol 13: 281–292. https://doi.org/10.1071/PP9860281.

Evans JR, Von Caemmerer S (2013) Temperature response of carbon isotope discrimination and mesophyll conductance in tobacco. Plant Cell Environ 36: 745–756. https://doi.org/10.1111/j.1365-3040.2012.02591.x.

FAO–UNESCO (1990) Soil map of the world, revised legend. World Soil Resources Report 60. FAO, Rome, Italy. http://www.fao.org/soils-portal/data-hub/soil-classification/world-reference-base/en/. Accessed 30 November 2022

Farquhar GD (1983) On the nature of carbon isotope discrimination in C4 species. Funct Plant Biol 10: 205–226. https://doi.org/10.1071/PP9830205.

Farquhar GD, Cernusak LA (2012) Ternary effects on the gas exchange of isotopologues of carbon dioxide. Plant Cell Environ 35: 1221–1231. https://doi.org/10.1111/j.1365-3040.2012.02484.x.

Farquhar GD, O'Leary MH, Berry JA (1982) On the relationship between carbon isotope discrimination and the intercellular carbon dioxide concentration in leaves. Funct Plant Biol 9: 121–127. https://doi.org/10.1071/PP9820121.

February EC, Higgins SI (2016) Rapid leaf deployment strategies in a deciduous savanna. PLoS ONE 11, article id 0157833. https://doi:10.1371/journal.pone.0157833.

Fischer S, Hanf S, Frosch T, Gleixner G, Popp J, Trumbore S, Hartmann H (2015) *Pinus sylvestris* switches respiration substrates under shading but not during drought. New Phytol 207: 542–550. https://doi.org/10.1111/nph.13452.

Flexas J, Ribas-Carbó M, Diaz-Espejo A, Galmés J, Medrano H (2008) Mesophyll conductance to CO_2: current knowledge and future prospects. Plant Cell Environ 31: 602–621. https://doi.org/10.1111/j.1365-3040.2007.01757.x.

Fonti M, Vaganov E, Wirth C, Shashkin A, Astrakhantseva N, Schulze E-D (2018) Age-effect on intra-annual $\delta^{13}C$-variability within Scots pine tree-rings from central Siberia. Forests 9, article id 364. https://doi:10.3390/f9060364.

Frank DC, Poulter B, Saurer M, Esper J, Huntingford C, Helle G, Treydte K, Zimmermann NE, Schleser GH, Ahlström A, Ciais P, Friedlingstein P, Levis S, Lomas M, Sitch S, Viovy N, Andreu-Hayles L, Bednarz Z, Berninger F, Boettger T, D'Alessandro CM, Daux V, Filot M, Grabner M, Gutierrez E, Haupt M, Hilasvuori E, Jungner H, Kalela-Brundin M, Krapiec M, Leuenberger M, Loader NJ, Marah H, Masson-Delmotte V, Pazdur A, Pawelczyk S, Pierre M, Planells O, Pukiene R, Reynolds-Henne CE, Rinne KT, Saracino A, Sonninen E, Stievenard M, Switsur VR, Szczepanek M, Szychowska-Krapiec E, Todaro L, Waterhouse JS, Weigl M (2015) Water-use efficiency and transpiration across European forests during the Anthropocene. Nature Clim Change 5: 579–583. https://doi.org/10.1038/nclimate2614.

Galiano L, Timofeeva G, Saurer M, Siegwolf R, Martínez-Vilalta J, Hommel R, Gessler A (2017) The fate of recently fixed carbon after drought release: towards unravelling C storage regulation in *Tilia platyphyllos* and *Pinus sylvestris*. Plant Cell Environ 40: 1711–1724. https://doi.org/10.1111/pce.12972.

Gaudinski JB, Torn MS, Riley WJ, Swanston C, Trumbore SE, Joslin JD, Majdi H, Dawson TE, Hanson PJ (2009) Use of stored carbon reserves in growth of temperate tree roots and leaf buds: analyses using radiocarbon measurements and modeling. Glob Change Biol 15: 992–1014. https://doi.org/10.1111/j.1365-2486.2008.01736.x.

Gauthier S, Bernier P, Kuuluvainen T, Shvidenko AZ, Schepaschenko DG (2015) Boreal forest health and global change. Science 349: 819–822. https://doi.org/10.1126/science.aaa9092.

Gessler A, Brandes E, Buchmann N, Helle G, Rennenberg H, Barnard RL (2009b) Tracing carbon and oxygen isotope signals from newly assimilated sugars in the leaves to the tree-ring archive. Plant Cell Environ 32: 780–795. https://doi.org/10.1111/j.1365-3040.2009.01957.x.

Gessler A, Ferrio JP (2022) Chapter 13: Postphotosynthetic fractionation in leaves, phloem and stem. In: Siegwolf RTW, Brooks JR, Roden J, Saurer M (eds) Stable isotopes in tree rings. Tree Physiol, pp 381–396. https://doi:10.1007/978-3-030-92698-4_13

Gessler A, Ferrio JP, Hommel R, Treydte K, Werner RA, Monson RK (2014) Stable isotopes in tree rings: towards a mechanistic understanding of isotope fractionation and mixing processes from the leaves to the wood. Tree Physiol 34: 796–818. https://doi.org/10.1093/treephys/tpu040.

Gessler A, Keitel C, Kodama N, Weston C, Winters AJ, Keith H, Grice K, Leuning R, Farquhar GD (2007) $\delta^{13}C$ of organic matter transported from the leaves to the roots in *Eucalyptus delegatensis*: short-term variations and relation to respired CO_2. Functional Plant Biol 34: 692–706. https://doi.org/10.1071/FP07064.

Gessler A, Tcherkez G, Karyanto O, Keitel C, Ferrio JP, Ghashghaie J, Kreuzwieser J, Farquhar GD (2009a) On the metabolic origin of the carbon isotope composition of CO_2 evolved from darkened light-acclimated leaves in *Ricinus communis*. New Phytol 181: 374–386. https://doi.org/10.1111/j.1469-8137.2008.02672.x.

Gessler A, Tcherkez G, Peuke AD, Ghashghaie J, Farquhar GD (2008) Experimental evidence for diel variations of the carbon isotope composition in leaf, stem and phloem sap organic matter in *Ricinus communis*. Plant Cell Environ 31: 941–953. https://doi.org/10.1111/j.1365-3040.2008.01806.x.

Ghashghaie J, Badeck F-W, Lanigan G, Nogués S, Tcherkez G, Deléens E, Cornic G, Griffiths H (2003) Carbon isotope fractionation during dark respiration and photorespiration in C3 plants. Phytochem Rev 2: 145–161. https://doi.org/10.1023/B:PHYT.0000004326.00711.ca.

Gilbert A, Robins RJ, Remaud GS, Tcherkez GGB (2012) Intramolecular ^{13}C pattern in hexoses from autotrophic and heterotrophic C3 plant tissues. P Natl Acad Sci USA 109: 18204–18209. https://doi.org/10.1073/pnas.1211149109.

Gimeno TE, Campany CE, Drake JE, Barton CVM, Tjoelker MG, Ubierna N, Marshall JD (2021) Whole-tree mesophyll conductance reconciles isotopic and gas-exchange estimates of water-use efficiency. New Phytol 229: 2535–2547. https://doi.org/10.1111/nph.17088.

Gleixner G, Schmidt H-L (1997) Carbon isotope effects on the fructose-1,6-bisphosphate aldolase reaction, origin for non-statistical ^{13}C distributions in carbohydrates. J Biol Chem 272: 5382–5387. https://doi.org/10.1074/jbc.272.9.5382.

Gleixner G, Scrimgeour C, Schmidt HL, Viola R (1998) Stable isotope distribution in the major metabolites of source and sink organs of *Solanum tuberosum* L.: a powerful tool in the study of metabolic partitioning in intact plants. Planta 207: 241–245. https://doi.org/10.1007/s004250050479.

Guérard N, Maillard P, Bréchet C, Lieutier F, Dreyer E (2007) Do trees use reserve or newly assimilated carbon for their defense reactions? A ^{13}C labeling approach with young Scots pines inoculated with a bark-beetle-associated fungus (*Ophiostoma brunneo ciliatum*). Ann For Sci 64: 601–608. https://doi.org/10.1051/forest:2007038.

Guy RD, Vanlerberghe GC, Turpin DH (1989) Significance of phospho*enol*pyruvate carboxylase during ammonium assimilation. Plant Physiol 89: 1150–1157. https://doi.org/10.1104/pp.89.4.1150.

Hanf S, Fischer S, Hartmann H, Keiner R, Trumbore S, Popp J, Frosch T (2015) Online investigation of respiratory quotients in *Pinus sylvestris* and *Picea abies* during drought and shading by means of cavity-enhanced Raman multi-gas spectrometry. Analyst 140: 4473–4481. https://doi.org/10.1039/C5AN00402K.

Hartmann H, Trumbore S (2016) Understanding the roles of nonstructural carbohydrates in forest trees – from what we can measure to what we want to know. New Phytol 211: 386–403. https://doi.org/10.1111/nph.13955.

Hartmann H, Ziegler W, Trumbore S (2013) Lethal drought leads to reduction in nonstructural carbohydrates in Norway spruce tree roots but not in the canopy. Funct Ecol 27: 413–427. https://doi.org/10.1111/1365-2435.12046.

Helama S, Arppe L, Timonen M, Mielikäinen K, Oinonen M (2018) A 7.5 ka chronology of stable carbon isotopes from tree rings with implications for their use in palaeo-cloud reconstruction. Glob Planet Change 170: 20–33. https://doi.org/10.1016/j.gloplacha.2018.08.002.

Helle G, Schleser GH (2004) Beyond CO_2-fixation by Rubisco – an interpretation of $^{13}C/^{12}C$ variations in tree rings from novel intra-seasonal studies on broad-leaf trees. Plant Cell Environ 27: 367–380. https://doi.org/10.1111/j.0016-8025.2003.01159.x.

Hobbie EA, Werner RA (2004) Intramolecular, compound-specific, and bulk carbon isotope patterns in C_3 and C_4 plants: a review and synthesis. New Phytol 161: 371–385. https://doi.org/10.1111/j.1469-8137.2004.00970.x.

Hymus GJ, Maseyk K, Valentini R, Yakir D (2005) Large daily variation in ^{13}C-enrichment of leaf-respired CO_2 in two *Quercus* forest canopies. New Phytol 167: 377–384. https://doi.org/10.1111/j.1469-8137.2005.01475.x.

Igamberdiev AU, Mikkelsen TN, Ambus P, Bauwe H, Lea PJ, Gardeström P (2004) Photorespiration contributes to stomatal regulation and carbon isotope fractionation: a study with barley, potato and *Arabidopsis* plants deficient in glycine decarboxylase. Photosynth Res 81: 139–152. https://doi.org/10.1023/B:PRES.0000035026.05237.ec.

Jäggi M, Saurer M, Fuhrer J, Siegwolf R (2002) The relationship between the stable carbon isotope composition of needle bulk material, starch, and tree rings in *Picea abies*. Oecologia 131: 325–332. https://doi.org/10.1007/s00442-002-0881-0.

Jokinen P, Pirinen P, Kaukoranta JP, Kangas A, Alenius P, Eriksson P, Johansson M, Wilkman S (2021) Climatological and oceanographic statistics of Finland 1991–2020. Finnish Meteorological Institute, Helsinki, Finland. https://doi.org/10.35614/isbn.9789523361485. Accessed 16 November 2022.

Julius BT, Leach KA, Tran TM, Mertz RA, Braun DM (2017) Sugar transporters in plants: new insights and discoveries. Plant Cell Physiol 58: 1442–1460. https://doi.org/10.1093/pcp/pcx090.

Jyske T, Mäkinen H, Kalliokoski T, Nöjd P (2014) Intra-annual tracheid production of Norway spruce and Scots pine across a latitudinal gradient in Finland. Agric For Meteorol 194: 241–254. https://doi.org/10.1093/pcp/pcx090.

Kagawa A (2003) Effects of spatial and temporal variability in soil moisture on widths and $\delta^{13}C$ values of eastern Siberian tree rings. J Geophys Res 108, article id 4500. https://doi:10.1029/2002JD003019.

Kagawa A, Sugimoto A, Maximov TC (2006) Seasonal course of translocation, storage and remobilization of ^{13}C pulse-labeled photoassimilate in naturally growing *Larix gmelinii* saplings. New Phytol 171: 793–804. https://doi.org/10.1111/j.1469-8137.2006.01780.x.

Kauppi PE, Posch M, Pirinen P (2014) Large impacts of climatic warming on growth of boreal forests since 1960. PLoS ONE 9, article id 111340. https://10.1371/journal.pone.0111340.

Keenan TF, Migliavacca M, Papale D, Baldocchi D, Reichstein M, Torn M, Wutzler T (2019) Widespread inhibition of daytime ecosystem respiration. Nat Ecol Evol 3: 407–415. https://doi.org/10.1038/s41559-019-0809-2.

Keitel C, Adams MA, Holst T, Matzarakis A, Mayer H, Rennenberg H, GEßLER A (2003) Carbon and oxygen isotope composition of organic compounds in the phloem sap provides a short-term measure for stomatal conductance of European beech (*Fagus sylvatica* L.). Plant Cell Environ 26: 1157–1168. https://doi.org/10.1046/j.1365-3040.2003.01040.x.

Klumpp K, Schaufele R, Lotscher M, Lattanzi FA, Feneis W, Schnyder H (2005) C-isotope composition of CO_2 respired by shoots and roots: fractionation during dark respiration? Plant Cell Environ 28: 241–250. https://doi.org/10.1111/j.1365-3040.2004.01268.x.

Knauer J, Zaehle S, Medlyn BE, Reichstein M, Williams CA, Migliavacca M, De Kauwe MG, Werner C, Keitel C, Kolari P, Limousin J, Linderson M (2018) Towards physiologically meaningful water-use efficiency estimates from eddy covariance data. Glob Change Biol 24: 694–710. https://doi.org/10.1111/gcb.13893.

Kodama N, Barnard RL, Salmon Y, Weston C, Ferrio JP, Holst J, Werner RA, Saurer M, Rennenberg H, Buchmann N, Gessler A (2008) Temporal dynamics of the carbon isotope composition in a *Pinus sylvestris* stand: from newly assimilated organic carbon to respired carbon dioxide. Oecologia 156: 737–750. https://doi.org/10.1007/s00442-008-1030-1.

Kolari P, Aalto J, Levula J, Kulmala L, Ilvesniemi H, Pumpanen J (2022) SMEAR II Hyytiälä site characteristics. https://doi.org/10.5281/zenodo.5909681. Accessed January 27 2022

Kolari P, Bäck J, Taipale R, Ruuskanen TM, Kajos MK, Rinne J, Kulmala M, Hari P (2012) Evaluation of accuracy in measurements of VOC emissions with dynamic chamber system. Atmos Environ 62: 344–351. https://doi.org/10.1016/j.atmosenv.2012.08.054.

Kolari P, Kulmala L, Pumpanen J, Launiainen S, Ilvesniemi H, Hari P, Nikinmaa E (2009) CO_2 exchange and component CO_2 fluxes of a boreal Scots pine forest. Boreal Environ Res 14: 761–783.

Köster E, Köster K, Berninger F, Pumpanen J (2015) Carbon dioxide, methane and nitrous oxide fluxes from podzols of a fire chronosequence in the boreal forests in Värriö, Finnish Lapland. Geoderma Reg 5: 181–187. https://doi.org/10.1016/j.geodrs.2015.07.001.

Köster K, Berninger F, Lindén A, Köster E, Pumpanen J (2014) Recovery in fungal biomass is related to decrease in soil organic matter turnover time in a boreal fire chronosequence. Geoderma 235–236: 74–82. https://doi.org/10.1016/j.geoderma.2014.07.001.

Kouchi H, Yoneyama T (1984) Dynamics of carbon photosynthetically assimilated in nodulated soya bean plants under steady-state conditions 2. The incorporation of ^{13}C into carbohydrates, organic acids, amino acids and some storage compounds. Ann Bot 53: 883–896. https://doi.org/10.1093/oxfordjournals.aob.a086758.

Krummen M, Hilkert AW, Juchelka D, Duhr A, Schlüter H-J, Pesch R (2004) A new concept for isotope ratio monitoring liquid chromatography/mass spectrometry. Rapid Commun Mass Spectrom 18: 2260–2266. https://doi.org/10.1002/rcm.1620.

Kulmala L, Launiainen S, Pumpanen J, Lankreijer H, Lindroth A, Hari P, Vesala T (2008) H_2O and CO_2 fluxes at the floor of a boreal pine forest. Tellus B: Chem Phys Meteorol 60: 167–178. https://doi.org/10.1111/j.1600-0889.2007.00327.x.

Kulmala L, Pumpanen J, Kolari P, Dengel S, Berninger F, Köster K, Matkala L, Vanhatalo A, Vesala T, Bäck J (2019) Inter- and intra-annual dynamics of photosynthesis differ between forest floor vegetation and tree canopy in a subarctic Scots pine stand. Agric For Meteorol 271: 1–11. https://doi.org/10.1016/j.agrformet.2019.02.029.

Lanigan GJ, Betson N, Griffiths H, Seibt U (2008) Carbon isotope fractionation during photorespiration and carboxylation in *Senecio*. Plant Physiol 148: 2013–2020. https://doi.org/10.1104/pp.108.130153.

Lapenis A, Shvidenko A, Shepaschenko D, Nilsson S, Aiyyer A (2005) Acclimation of Russian forests to recent changes in climate. Glob Change Biol 11: 2090–2102. https://doi.org/10.1111/j.1365-2486.2005.001069.x.

Le Roux X, Bariac T, Sinoquet H, Genty B, Piel C, Mariotti A, Girardin C, Richard P (2001) Spatial distribution of leaf water-use efficiency and carbon isotope discrimination within an isolated tree crown. Plant Cell Environ 24: 1021–1032. https://doi.org/10.1046/j.0016-8025.2001.00756.x.

Leavitt SW, Long A (1984) Sampling strategy for stable carbon isotope analysis of tree rings in pine. Nature 311: 145–147. https://doi.org/10.1038/311145a0.

Lehmann MM, Ghiasi S, George GM, Cormier M-A, Gessler A, Saurer M, Werner RA (2019) Influence of starch deficiency on photosynthetic and post-photosynthetic carbon isotope fractionations. J Exp Bot 70: 1829–1841. https://doi.org/10.1093/jxb/erz045.

Li M, Zhu J (2011) Variation of $\delta^{13}C$ of wood and foliage with canopy height differs between evergreen and deciduous species in a temperate forest. Plant Ecol 212: 543–551. https://doi.org/10.1007/s11258-010-9843-5.

Liu Y, Ta W, Li Q, Song H, Sun C, Cai Q, Liu H, Wang L, Hu S, Sun J, Zhang W, Li W (2018) Tree-ring stable carbon isotope-based April–June relative humidity reconstruction since AD 1648 in Mt. Tianmu, China. Clim Dyn 50: 1733–1745. https://doi.org/10.1007/s00382-017-3718-6.

Loader NJ, McCarroll D, Barker S, Jalkanen R, Grudd H (2017) Inter-annual carbon isotope analysis of tree-rings by laser ablation. Chem Geol 466: 323–326. https://doi.org/10.1016/j.chemgeo.2017.06.021.

Loader NJ, Robertson I, Barker AC, Switsur VR, Waterhouse J (1997) An improved technique for the batch processing of small wholewood samples to α-cellulose. Chem Geol 136: 313–317. https://doi.org/10.1016/S0009-2541(96)00133-7.

Ma WT, Tcherkez G, Wang XM, Schäufele R, Schnyder H, Yang Y, Gong XY (2021) Accounting for mesophyll conductance substantially improves ^{13}C-based estimates of intrinsic water-use efficiency. New Phytol 229: 1326–1338. https://doi.org/10.1111/nph.16958.

Mathias JM, Thomas RB (2021) Global tree intrinsic water use efficiency is enhanced by increased atmospheric CO_2 and modulated by climate and plant functional types. P Natl Acad Sci USA 118, article id 2014286118. https://doi.org/10.1073/pnas.2014286118.

Maunoury F, Berveiller D, Lelarge C, Pontailler J-Y, Vanbostal L, Damesin C (2007) Seasonal, daily and diurnal variations in the stable carbon isotope composition of carbon dioxide respired by tree trunks in a deciduous oak forest. Oecologia 151: 268–279. https://doi.org/10.1007/s00442-006-0592-z.

Mauve C, Bleton J, Bathellier C, Lelarge-Trouverie C, Guérard F, Ghashghaie J, Tchapla A, Tcherkez G (2009) Kinetic $^{12}C/^{13}C$ isotope fractionation by invertase: evidence for a small *in vitro* isotope effect and comparison of two techniques for the isotopic analysis of carbohydrates. Rapid Commun Mass Spectrom 23: 2499–2506. https://doi.org/10.1002/rcm.4068.

McCarroll D, Whitney M, Young GHF, Loader NJ, Gagen MH (2017) A simple stable carbon isotope method for investigating changes in the use of recent versus old carbon in oak. Tree Physiol 37: 1021–1027. https://doi.org/10.1093/treephys/tpx030.

Medlyn BE, De Kauwe MG, Lin Y, Knauer J, Duursma RA, Williams CA, Arneth A, Clement R, Isaac P, Limousin J, Linderson M, Meir P, Martin-StPaul N, Wingate L (2017) How do leaf and ecosystem measures of water-use efficiency compare? New Phytol 216: 758–770. https://doi.org/10.1111/nph.14626.

Merchant A, Wild B, Richter A, Bellot S, Adams MA, Dreyer E (2011) Compound-specific differences in ^{13}C of soluble carbohydrates in leaves and phloem of 6-month-old *Eucalyptus globulus* (Labill). Plant Cell Environ 34: 1599–1608. https://doi.org/10.1111/j.1365-3040.2011.02359.x.

Mook WG, Bommerson JC, Staverman WH (1974) Carbon isotope fractionation between dissolved bicarbonate and gaseous carbon dioxide. Earth Planet Sci Lett 22: 169–176. https://doi.org/10.1016/0012-821X(74)90078-8.

Muhr J, Trumbore S, Higuchi N, Kunert N (2018) Living on borrowed time – Amazonian trees use decade-old storage carbon to survive for months after complete stem girdling. New Phytol 220: 111–120. https://doi.org/10.1111/nph.15302.

Nadwodnik J, Lohaus G (2008) Subcellular concentrations of sugar alcohols and sugars in relation to phloem translocation in *Plantago major*, *Plantago maritima*, *Prunus persica*, and *Apium graveolens*. Planta 227: 1079–1089. https://doi.org/10.1007/s00425-007-0682-0.

Ogée J, Barbour MM, Wingate L, Bert D, Bosc A, Stievenard M, Lambrot C, Pierre M, Bariac T, Loustau D, Dewar RC (2009) A single-substrate model to interpret intra-annual stable isotope signals in tree-ring cellulose. Plant Cell Environ 32: 1071–1090. https://doi.org/10.1111/j.1365-3040.2009.01989.x.

Ogée J, Peylin P, Ciais P, Bariac T, Brunet Y, Berbigier P, Roche C, Richard P, Bardoux G, Bonnefond J-M (2003) Partitioning net ecosystem carbon exchange into net assimilation and respiration using $^{13}CO_2$ measurements: A cost-effective sampling strategy. Global Biogeochem Cycles 17, article id 1070. https://doi:10.1029/2002GB001995.

Ogée J, Wingate L, Genty B (2018) Estimating mesophyll conductance from measurements of $C^{18}OO$ photosynthetic discrimination and carbonic anhydrase activity. Plant Physiol 178: 728–752. https://doi.org/10.1104/pp.17.01031.

O'Leary MH (1984) Measurement of the isotope fractionation associated with diffusion of carbon dioxide in aqueous solution. J Phys Chem 88: 823–825. https://doi.org/10.1021/j150648a041.

Peng C, Ma Z, Lei X, Zhu Q, Chen H, Wang W, Liu S, Li W, Fang X, Zhou X (2011) A drought-induced pervasive increase in tree mortality across Canada's boreal forests. Nat Clim Change 1: 467–471. https://doi.org/10.1038/nclimate1293.

Pons TL, Flexas J, von Caemmerer S, Evans JR, Genty B, Ribas-Carbo M, Brugnoli E (2009) Estimating mesophyll conductance to CO_2: methodology, potential errors, and recommendations. J Exp Bot 60: 2217–2234. https://doi.org/10.1093/jxb/erp081.

Priault P, Wegener F, Werner C (2009) Pronounced differences in diurnal variation of carbon isotope composition of leaf respired CO_2 among functional groups. New Phytol 181: 400–412. https://doi.org/10.1111/j.1469-8137.2008.02665.x.

Rennie EA, Turgeon R (2009) A comprehensive picture of phloem loading strategies. P Natl Acad Sci USA 106: 14162–14167. https://doi.org/10.1073/pnas.0902279106.

Rinne KT, Saurer M, Kirdyanov AV, Bryukhanova MV, Prokushkin AS, Churakova Sidorova OV, Siegwolf RTW (2015b) Examining the response of needle carbohydrates from Siberian larch trees to climate using compound-specific $\delta^{13}C$ and concentration analyses. Plant Cell Environ 38: 2340–2352. https://doi.org/10.1111/pce.12554.

Rinne KT, Saurer M, Kirdyanov AV, Loader NJ, Bryukhanova MV, Werner RA, Siegwolf RTW (2015a) The relationship between needle sugar carbon isotope ratios and tree rings of larch in Siberia. Tree Physiol 35: 1192–1205. https://doi.org/10.1093/treephys/tpv096.

Rinne KT, Saurer M, Streit K, Siegwolf RTW (2012) Evaluation of a liquid chromatography method for compound-specific $\delta^{13}C$ analysis of plant carbohydrates in alkaline media: compound-specific $\delta^{13}C$ analysis of plant carbohydrates in alkaline media. Rapid Commun Mass Spectrom 26: 2173–2185. https://doi.org/10.1002/rcm.6334.

Rinne-Garmston KT, Helle G, Lehmann MM, Sahlstedt E, Schleucher J, Waterhouse J (2022) Chapter 7: Newer developments in tree-ring stable isotope methods. In: Siegwolf RTW, Brooks JR, Roden J, Saurer M (eds) Stable isotopes in tree rings. Tree Physiol, pp 215–249. https://doi:10.1007/978-3-030-92698-4_7.

Rinne-Garmston KT, Tang Y, Sahlstedt E, Adamczyk B, Saurer M, Salmon Y, Carrasco M del RD, Hölttä T, Lehmann MM, Mo L, Young G (in preparation) Drivers of intra-seasonal $\delta^{13}C$ signals in tree-rings of *Pinus sylvestris*.

Rissanen K, Vanhatalo A, Salmon Y, Bäck J, Hölttä T (2020) Stem emissions of monoterpenes, acetaldehyde and methanol from Scots pine (*Pinus sylvestris* L.) affected by tree–water relations and cambial growth. Plant Cell Environ 43: 1751–1765. https://doi.org/10.1111/pce.13778.

Rossi S, Anfodillo T, Menardi R (2006) Trephor: A new tool for sampling microcores from tree stems. IAWA J, 27: 89–97. https://doi.org/10.1163/22941932-90000139.

Rossmann A, Butzenlechner M, Schmidt HL (1991) Evidence for a nonstatistical carbon isotope distribution in natural glucose. Plant Physiol 96: 609–614. https://doi.org/10.1104/pp.96.2.609.

Rumman R, Atkin OK, Bloomfield KJ, Eamus D (2018) Variation in bulk-leaf ^{13}C discrimination, leaf traits and water-use efficiency–trait relationships along a continental-scale climate gradient in Australia. Glob Change Biol 24: 1186–1200. https://doi.org/10.1111/gcb.13911.

Schiestl-Aalto P, Kulmala L, Mäkinen H, Nikinmaa E, Mäkelä A (2015) CASSIA – a dynamic model for predicting intra-annual sink demand and interannual growth variation in Scots pine. New Phytol 206: 647–659. https://doi.org/10.1111/nph.13275.

Schiestl-Aalto P, Ryhti K, Mäkelä A, Peltoniemi M, Bäck J, Kulmala L (2019) Analysis of the NSC storage dynamics in tree organs reveals the allocation to belowground symbionts in the framework of whole tree carbon balance. Front For Glob Change 2, article id 17. https://doi:10.3389/ffgc.2019.00017.

Schiestl-Aalto P, Stangl ZR, Tarvainen L, Wallin G, Marshall J, Mäkelä A (2021) Linking canopy-scale mesophyll conductance and phloem sugar $\delta^{13}C$ using empirical and modelling approaches. New Phytol 229: 3141–3155. https://doi.org/10.1111/nph.17094.

Schleser GH (1990) Investigations of the $\delta^{13}C$ Pattern in Leaves of *Fagus sylvatica* L. J Exp Bot 41: 565–572. https://doi.org/10.1093/jxb/41.5.565.

Schubert BA, Jahren AH (2018) Incorporating the effects of photorespiration into terrestrial paleoclimate reconstruction. Earth-Sci Rev 177: 637–642. https://doi.org/10.1016/j.earscirev.2017.12.008.

Schulze B, Wirth C, Linke P, Brand WA, Kuhlmann I, Horna V, Schulze E-D (2004) Laser ablation-combustion-GC-IRMS – a new method for online analysis of intra-annual variation of ^{13}C in tree rings. Tree Physiol 24: 1193–1201. https://doi.org/10.1093/treephys/24.11.1193.

Seibt U, Rajabi A, Griffiths H, Berry JA (2008) Carbon isotopes and water use efficiency: sense and sensitivity. Oecologia 155: 441–454. https://doi.org/10.1007/s00442-007-0932-7.

Shrestha A, Song X, Barbour MM (2019) The temperature response of mesophyll conductance, and its component conductances, varies between species and genotypes. Photosynth Res 141: 65–82. https://doi.org/10.1007/s11120-019-00622-z.

Skomarkova MV, Vaganov EA, Mund M, Knohl A, Linke P, Boerner A, Schulze E-D (2006) Inter-annual and seasonal variability of radial growth, wood density and carbon isotope ratios in tree rings of beech (*Fagus sylvatica*) growing in Germany and Italy. Trees 20: 571–586. https://doi.org/10.1007/s00468-006-0072-4.

Smith M, Wild B, Richter A, Simonin K, Merchant A (2016) Carbon isotope composition of carbohydrates and polyols in leaf and phloem sap of *Phaseolus vulgaris* L. influences predictions of plant water use efficiency. Plant Cell Physiol 57: 1756–1766. https://doi.org/10.1093/pcp/pcw099.

Soudant A, Loader NJ, Bäck J, Levula J, Kljun N (2016) Intra-annual variability of wood formation and $\delta^{13}C$ in tree-rings at Hyytiälä, Finland. Agric For Meteorol 224: 17–29. https://doi.org/10.1016/j.agrformet.2016.04.015.

Stangl ZR, Tarvainen L, Wallin G, Ubierna N, Räntfors M, Marshall JD (2019) Diurnal variation in mesophyll conductance and its influence on modelled water-use efficiency in a mature boreal *Pinus sylvestris* stand. Photosynth Res 141: 53–63. https://doi.org/10.1007/s11120-019-00645-6.

Stokes VJ, Morecroft MD, Morison JIL (2010) Comparison of leaf water use efficiency of oak and sycamore in the canopy over two growing seasons. Trees 24: 297–306. https://doi.org/10.1007/s00468-009-0399-8.

Streeter JG, Lohnes DG, Fioritto RJ (2001) Patterns of pinitol accumulation in soybean plants and relationships to drought tolerance. Plant Cell Environ 24: 429–438. https://doi.org/10.1046/j.1365-3040.2001.00690.x.

Streit K, Rinne KT, Hagedorn F, Dawes MA, Saurer M, Hoch G, Werner RA, Buchmann N, Siegwolf RTW (2012) Tracing fresh assimilates through *Larix decidua* exposed to elevated CO_2 and soil warming at the alpine treeline using compound-specific stable isotope analysis. New Phytol 197: 838–849. https://doi.org/10.1111/nph.12074.

Sun W, Resco V, Williams DG (2012) Environmental and physiological controls on the carbon isotope composition of CO_2 respired by leaves and roots of a C3 woody legume (*Prosopis velutina*) and a C4 perennial grass (*Sporobolus wrightii*). Plant Cell Environ 35: 567–577. https://doi.org/10.1111/j.1365-3040.2011.02436.x.

Tarin T, Nolan RH, Medlyn BE, Cleverly J, Eamus D (2020) Water-use efficiency in a semi-arid woodland with high rainfall variability. Glob Change Biol 26: 496–508. https://doi.org/10.1111/gcb.14866.

Tcherkez G (2006) How large is the carbon isotope fractionation of the photorespiratory enzyme glycine decarboxylase? Funct Plant Biol 33: 911–920. https://doi.org/10.1071/FP06098.

Tcherkez G, Farquhar G, Badeck F, Ghashghaie J (2004) Theoretical considerations about carbon isotope distribution in glucose of C3 plants. Functional Plant Biol 31: 857–877. https://doi.org/10.1071/FP04053.

Tcherkez G, Mahé A, Hodges M (2011) $^{12}C/^{13}C$ fractionations in plant primary metabolism. Trends Plant Sci 16: 499–506. https://doi.org/10.1016/j.tplants.2011.05.010.

Tcherkez G, Schäufele R, Nogués S, Piel C, Boom A, Lanigan G, Barbaroux C, Mata C, Elhani S, Hemming D, Maguas C, Yakir D, Badeck FW, Griffiths H, Schnyder H, Ghashghaie J (2010) On the $^{12}C/^{13}C$ isotopic signal of day and night respiration at the mesocosm level. Plant Cell Environ 33: 900–913. https://doi.org/10.1111/j.1365-3040.2010.02115.x.

Ubierna N, Gandin A, Boyd RA, Cousins AB (2017) Temperature response of mesophyll conductance in three C_4 species calculated with two methods: ^{18}O discrimination and *in vitro* V_{pmax}. New Phytol 214: 66–80. https://doi.org/10.1111/nph.14359.

Uddling J, Wallin G (2012) Interacting effects of elevated CO_2 and weather variability on photosynthesis of mature boreal Norway spruce agree with biochemical model predictions. Tree Physiol 32: 1509–1521. https://doi.org/10.1093/treephys/tps086.

Vaganov EA, Schulze E-D, Skomarkova MV, Knohl A, Brand WA, Roscher C (2009) Intra-annual variability of anatomical structure and $\delta^{13}C$ values within tree rings of spruce and pine in alpine, temperate and boreal Europe. Oecologia 161: 729–745. https://doi.org/10.1007/s00442-009-1421-y.

Vesala T, Suni T, Rannik Ü, Keronen P, Markkanen T, Sevanto S, Grönholm T, Smolander S, Kulmala M, Ilvesniemi H, Ojansuu R, Uotila A, Levula J, Mäkelä A, Pumpanen J, Kolari P, Kulmala L, Altimir N, Berninger F, Nikinmaa E, Hari P (2005) Effect of thinning on surface fluxes in a boreal forest. Global Biogeochem Cycles 19, article id GB2001. https://doi:10.1029/2004GB002316.

Villar-Salvador P, Uscola M, Jacobs DF (2015) The role of stored carbohydrates and nitrogen in the growth and stress tolerance of planted forest trees. New For 46: 813–839. https://doi.org/10.1007/s11056-015-9499-z.

Vincent-Barbaroux C, Berveiller D, Lelarge-Trouverie C, Maia R, Máguas C, Pereira J, Chaves MM, Damesin C (2019) Carbon-use strategies in stem radial growth of two oak species, one Temperate deciduous and one Mediterranean evergreen: what can be inferred from seasonal variations in the $\delta^{13}C$ of the current year ring? Tree Physiol 39: 1329–1341. https://doi.org/10.1093/treephys/tpz043.

von Caemmerer S, Evans JR (2015) Temperature responses of mesophyll conductance differ greatly between species. Plant Cell Environ 38: 629–637. https://doi.org/10.1111/pce.12449.

von Felten S, Hättenschwiler S, Saurer M, Siegwolf R (2007) Carbon allocation in shoots of alpine treeline conifers in a CO_2 enriched environment. Trees 21: 283–294. https://doi.org/10.1007/s00468-006-0118-7.

Voronin V, Ivlev AA, Oskolkov V, Boettger T (2012) Intra-seasonal dynamics in metabolic processes of $^{13}C/^{12}C$ and $^{18}O/^{16}O$ in components of Scots pine twigs from southern Siberia

interpreted with a conceptual framework based on the Carbon Metabolism Oscillatory Model. BMC Plant Biol 12, article id 76. https://doi:10.1186/1471-2229-12-76.

Wanek W, Heintel S, Richter A (2001) Preparation of starch and other carbon fractions from higher plant leaves for stable carbon isotope analysis. Rapid Commun Mass Spectrom 15: 1136–1140. https://doi.org/10.1002/rcm.353.

Wang Y, Mao Z, Bakker MR, Kim JH, Brancheriau L, Buatois B, Leclerc R, Selli L, Rey H, Jourdan C, Stokes A (2018) Linking conifer root growth and production to soil temperature and carbon supply in temperate forests. Plant Soil 426: 33–50. https://doi.org/10.1007/s11104-018-3596-7.

Wehr R, Munger JW, McManus JB, Nelson DD, Zahniser MS, Davidson EA, Wofsy SC, Saleska SR (2016) Seasonality of temperate forest photosynthesis and daytime respiration. Nature 534: 680–683. https://doi.org/10.1038/nature17966.

Werner C, Wegener F, Unger S, Nogués S, Priault P (2009) Short-term dynamics of isotopic composition of leaf-respired CO_2 upon darkening: measurements and implications. Rapid Commun Mass Spectrom 23: 2428–2438. https://doi.org/10.1002/rcm.4036.

Wingate L, Ogée J, Burlett R, Bosc A, Devaux M, Grace J, Loustau D, Gessler A (2010) Photosynthetic carbon isotope discrimination and its relationship to the carbon isotope signals of stem, soil and ecosystem respiration. New Phytol 188: 576–589. https://doi.org/10.1111/j.1469-8137.2010.03384.x.

Wingate L, Seibt U, Moncrieff JB, Jarvis PG, Lloyd J (2007) Variations in ^{13}C discrimination during CO_2 exchange by *Picea sitchensis* branches in the field. Plant Cell Environ 30: 600–616. https://doi.org/10.1111/j.1365-3040.2007.01647.x.

Wingler A, Lea PJ, Quick WP, Leegood RC (2000) Photorespiration: metabolic pathways and their role in stress protection. Philos Trans R Soc Lond Ser B Biol Sci 355: 1517–1529. https://doi.org/10.1098/rstb.2000.0712.

Xu Q, Yin S, Ma Y, Song M, Song Y, Mu S, Li Y, Liu X, Ren Y, Gao C, Chen S, Liesche J (2020) Carbon export from leaves is controlled via ubiquitination and phosphorylation of sucrose transporter SUC2. P Natl Acad Sci USA 117: 6223–6230. https://doi.org/10.1073/pnas.1912754117.

Yang J, Medlyn BE, De Kauwe MG, Duursma RA, Jiang M, Kumarathunge D, Crous KY, Gimeno TE, Wujeska-Klause A, Ellsworth DS (2020) Low sensitivity of gross primary production to elevated CO_2 in a mature eucalypt woodland. Biogeosciences 17: 265–279. https://doi.org/10.5194/bg-2019-272.

Yi K, Maxwell JT, Wenzel MK, Roman DT, Sauer PE, Phillips RP, Novick KA (2019) Linking variation in intrinsic water-use efficiency to isohydricity: a comparison at multiple spatiotemporal scales. New Phytol 221:195–208. https://doi.org/10.1111/nph.15384.

Young GHF, Gagen MH, Loader NJ, McCarroll D, Grudd H, Jalkanen R, Kirchhefer A, Robertson I (2019) Cloud cover feedback moderates Fennoscandian summer temperature changes over the past 1000 years. Geophys Res Lett 46: 2811–2819. https://doi.org/10.1029/2018GL081046.

Zeide B (1993) Analysis of growth equations. For Sci 39: 594–616. https://doi.org/10.1093/forestscience/39.3.594.

Zeng X, Liu X, Treydte K, Evans MN, Wang W, An W, Sun W, Xu G, Wu G, Zhang X (2017) Climate signals in tree-ring $\delta^{18}O$ and $\delta^{13}C$ from southeastern Tibet: insights from observations and forward modelling of intra- to interdecadal variability. New Phytol 216: 1104–1118. https://doi.org/10.1111/nph.14750.

Zhang Q, Ficklin DL, Manzoni S, Wang L, Way D, Phillips RP, Novick KA (2019) Response of ecosystem intrinsic water use efficiency and gross primary productivity to rising vapor pressure deficit. Environ Res Lett 14, article id 074023. https://doi:10.1088/1748-9326/ab2603.